Since January 2020 Elsevier has created a COVID-19 resource centre with free information in English and Mandarin on the novel coronavirus COVID-19. The COVID-19 resource centre is hosted on Elsevier Connect, the company's public news and information website.

5.14 The Biophysics of Membrane Fusion

RN Collins, Cornell University, Ithaca, NY, USA
RW Holz, University of Michigan Medical School, MI, USA
J Zimmerberg, Eunice Kennedy Shriver National Institute of Child Health and Human Development, National Institutes of Health, Bethesda, MD, USA

Published by Elsevier B.V.

Abbreviations

6HB	six-helix bundle
GPI	glycerylphosphatidylinositol
PH	pleckstrin homology
SNAP-25	synaptosome-associated protein of 25 kD
SNARE	soluble *N*-ethylmaleimide-sensitive factor attachment protein (SNAP) receptor
TMD	transmembrane domain

The biological membrane is ancient, and crucial to the emergence of life itself. While a single topology of membrane was sufficient for bacteria and archebacteria, eukaryotic cells contain specialized subcellular systems of more topologies, enclosing many discontinuous volumes. In order to mix these intracellular volumes, and to secrete such volumes to the extracellular space, or to add a volume to the cytoplasmic space, the membranes enclosing one of these volumes must either rupture or merge with another membrane, a process termed membrane fusion. Topological membrane rearrangements, then, such as fusion, its inverse – fission, or formation of a membrane pore, are the most essential ingredients of the complex membrane dynamics of living cells. These membrane transformations are key elements of dynamic intracellular trafficking networks; they are also intimately linked to important pathological processes including cellular entry and egression of enveloped viruses and various parasites, membrane rupture and apoptosis. The topological membrane remodeling generally converges to highly bent intermediates. The characteristic length scales associated with key structural intermediates, such as fusion or fission pores, are typically of the order of tens of nanometers. It has become increasingly clear that critical properties of biological material at this nanoscale cannot be readily extrapolated from bulk measurements. Neither can they be obtained from experiments with individual molecules, as in many cases, especially in most membrane processes, the functional unit is not a single protein (e.g., channel), but a selectively self-assembled cluster of proteins and lipids acting in a highly co-operative manner. Therefore, for intuition and information about the nature of these transformations, we must create and study them where possible.

5.14.1 How Can We Study Membrane Fusion?

Since the biological membrane is thin (5 nm in thickness, that of two lipid molecules) we cannot see the process of membrane fusion under the microscope; we can only see the sequellae of fusion as organellar or cellular contents mix or are secreted. The simplest natural occurring instance of fusion is the coalescence of two miscible liquid droplets in air, whose two outer molecular layers merge into one. But these layers can dive into the interior, any given molecule is an ephemeral rather than integral part of the droplet's surface. Films made of soap or protein (e.g., bubbles made by children from detergent or blowing bubbles in their milk) provide a better model, and we have all seen them fuse and lyse before our eyes. However, they also have surfaces that can exchange with a bulky interior, and their width can vary. These films are unlike the biological membrane in that their apolar moities face the low dielectric air rather than the high dielectric watery interior of the film. The biological membrane is composed of lipids, proteins, and carbohydrates of varying chemical structure. It exists within the context of an aqueous cellular environment that prefers to avoid the interior of the membrane fusion. This entropically-driven hydrophobic effect leads to two important constraints on topological transformations, (1) a tension at the interface of the polar head groups of the lipids to resist any stretching, and (2) a uniform thickness which is primarily determined by the lipid constituents.

Bilayers made from phospholipids have been used extensively to study the fusion process, and more recently the fission process. Since the number of phospholipids molecules

far outnumber the other constituents, membrane entropy is dominated by the thermodynamics of the lipids themselves, and thus it is likely that whatever is learned from investigations of lipid bilayer fusion will inform us about biological membrane fusion. Indeed, it seems that many of the key intermediates of membrane fusion are the same in the fusion of synthetic and natural membranes.[1–3] We will not cover this ground, as many excellent reviews serve this purpose.[4–10] Rather, in this chapter we will introduce a number of controversies that the reader may be stimulated to solve.

5.14.2 Do Membranes Spontaneously Fuse?

In general there are a number of energy barriers that prevent fusion from proceeding spontaneously. First and foremost, there is the fact that in distilled water and dilute solutions of monovalent salt, all lipid bilayers resist close approach with a force that rises exponentially from an equilibrium distance of about 2 nm. With divalent cations in the solution bathing the membranes, close approach is possible, depending upon the lipid composition. This is readily seen as exchange of components in the contacting leaflets.[11,12] Presumably, this occurs through minute and transient contact sites in which the contacting leaflets are joined (hemifusion). However, this is not generally sufficient either for membrane fusion or the formation of an extended diaphragm composed of the outer, or non-contacting leaflets of the joining bilayers (termed hemifusion diaphragm),[13] for there are energetic restrictions to the widening of the hemifusion intermediate that joins the two leaflets (termed a stalk,[14–16]). The main way to facilitate the formation of a stable hemifusion diaphragm is to add hydrocarbon solvent to the membrane, so as to lower the energy of the three-way junction between the two bilayers and the joined diaphragm.[17,18]

Once there is a sufficient junction, another way to complete fusion is via the formation of a lipidic pore within the hemifusion diaphragm.[19] This can be facilitated by either increasing membrane tension, or by adding lipids whose composition favors spontaneous pore formation.[20,21] (Formally, such lipids would be defined as having positive monolayer spontaneous curvature.[22])

Thus it is possible to set up ionic and membrane compositional situations which allow the demonstration of membrane fusion and its intermediates without adding energy, thus spontaneous fusion is possible under a set of restricted conditions. What is not at all clear is the favorable effect of tension on the formation kinetics of hemifusion contacts, and how the huge hydration repulsion between contacting monolayers is breached during the tension-driven fusion of liposomes to bilayers.[20,23]

5.14.3 Is the Interior of The Fusion Pore Made of Protein or Lipid?

The fusion pore links the interior of a vesicle to the external space, or the interior of a virus to the cytoplasm. A relatively long-lived fusion pore is universal in biological fusion, regardless of whether exocytosis, viral fusion, or cell-cell fusion is studied. Since its discovery as a sub-ultrastructural entity, its architecture and composition has been in debate. In part, this is because of two very different views of the mechanism of membrane fusion: lipid centric and protein centric. In the lipid centric view, proteins surround a fusion site, and the conformational energy of the protein (as it transitions from a pre-fusion to a post-fusion form) is harnessed into stressing the encircled lipids to the point of a spontaneous transition in topology along a well-studied set of molecular intermediates, first a hemifusion intermediate – the stalk – and then the fusion pore (**Figure 1**).[21,24,25] The prediction of this hypothesis is clear: the proteins should be outside of an hourglass-shaped pore scaffolded by proteins. In the protein-centric view, proteins link up the two membranes that are to fuse and make a solid proteinaceous connection, a potential channel that is first closed, then opens to form the initial fusion pore.[3] The prediction of this hypothesis is also clear: the proteins should be at the center of the pore, surrounded and later infiltrated by lipids as the proteins dissociate to guide the topological change of the lipids. A direct method is needed to determine which of these predictions is met during different instances of biological fusion.

5.14.4 Why Is Synaptic Vesicle Fusion So Fast?

One of the abiding mysteries in biology is the great speed that synaptic transmission is capable of, with fusion of some vesicles beginning some tens of microseconds after Ca^{2+} floods the presynaptic intracellular release site.[26,27] This finding leads one to wonder if there is a physical state to a small population of vesicles whose fusion machinery is beyond the stages of priming and conformational change.[3,28] There are two main proposals:

1. that synaptotagmin provides positive curvature stress that translates into hemifusion at the center of a ring of protein at the base of a dimple,[29] and
2. that ring assemblies of SNARE (soluble *N*-ethylmaleimide-sensitive factor attachment protein (SNAP) receptor) and synaptotagmin complexes form to appropriately concentrate and orient C2b domains of synaptotagmin.[2]

This ring of ordered domains effectively creates a tube-like scaffold of positively charged protein residues that span the two membranes that are to fuse, a favorable location for dimples of membrane to approach each other. In other words, it would be an electrostatic tunnel for membrane fusion that is extended by the polybasic linker regions of syntaxin and synaptobrevin.[3] Variations of this model can account for many physiological pathways, including a small fraction of the vesicles that may already interacting at the level of the hemifusion prior to the entry of calcium. What is the role of calcium once it enters? First, Ca^{2+} turns on an 'electrostatic switch' initially proposed for synaptotagmin-syntaxin interaction, but better suited to instantaneously stressing the phospholipid bilayers of the presynaptic membrane and the synaptic vesicle for the ultra-rapid exocytosis seen in the nervous system. Second, even without synaptotagmin, Ca^{2+} speeds up fusion of SNARE-reconstituted membranes considerably. Perhaps divalent ions play a direct role, electrostatically complexing PS headgroups to promote fusion between negatively charged phospholipid bilayers. Is this

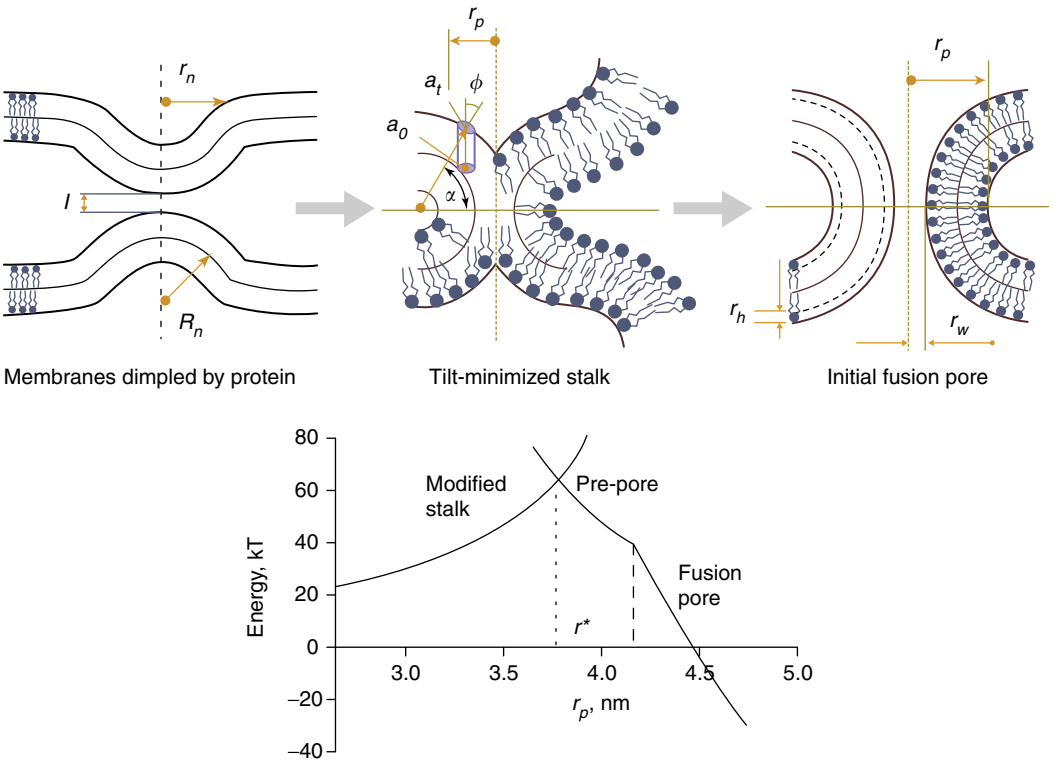

Figure 1 The cross-sections of energy-minimized structures for fusion of membranes deformed towards each other by proteins. Top, two membranes are deformed by fusogenic proteins that stress the bilayer by pulling the membranes together until they reach their hydration repulsion distance of *l*. The membrane forms hemispherical contact sites termed "dimples" for exocytosis or "nipples" for viral fusion. The next fusion intermediate is the stalk, shown here in a structure with the preceding constraints and using lipid tilt to minimize energy. Finally a fusion pore develops, after a poorly characterized transition state. Bottom, the calculated free energy of the above structures as a function of the radial development of either the stalk or the pore. Adapted from Kuzmin, P. I.; Zimmerberg, J.; Chizmadzhev, Y. A.; Cohen, F. S. A quantitative model for membrane fusion based on low-energy intermediates. *Proc. Natl. Acad. Sci. USA* **2001**, *98*, 7235–7240. Copyright by PNAS.

effect specific for calcium over magnesium? There are indications that the spontaneous curvature of PS in the presence of calcium, but not magnesium, is significantly more negative with calcium than with magnesium.[2] Ultimately, synaptotagmin, SNAREs, and the other proteins that comprise the exocytotic fusion machine must cajole lipids to move through a pathway that culminates in fusion pore opening. The SNARE proteins and synaptotagmin are the guides that walk and pull the membrane through a bumpy stalk-pore path, with electrostatic interactions playing a larger role than hitherto realized.[20]

5.14.5 Why Is PtdIns-4,5-P_2 Needed for Exocytotic Fusion?

Experiments on the permeabilized chromaffin cell established a requirement for ATP in membrane fusion in exocytotic secretion.[30,31] Further work revealed the product of ATP in exocytosis to be PtdIns-4,5-P_2, which stands out as a key player amongst bilayer lipids. It has been almost 20 years since this minor plasma membrane constituent was directly implicated in exocytosis. The early studies used biochemical approaches in permeabilized cells that directly implicated the polyphosphoinositides[30] and subsequently PIP kinase and PtdIns-4,5-P_2 5 as key components late in the fusion pathway. Imaging of PtdIns-4,5-P_2 in secreting cells demonstrates that the lipid is located on the plasma membrane and not on the secretory granule.[32,33] PtdIns-4,5-P_2 associates with syntaxin puncta in plasma membrane lawns from PC12 cells.[7] The concentration of PtdIns-4,5-P_2 in the cytoplasmic leaflet of puncta is surprisingly high, ~6 mole%.[8] An initial fusion pore of 3 nm diameter and 10 nm[9,10] would have room for approximately 140 phospholipid molecules (area = 70 Å^2) facing the cytosol including nine PtdIns-4,5-P_2 molecules at 6 mole%.

Clearly, PtdIns-4,5-P_2 is absolutely required for exocytosis. PtdIns-4,5-P_2 can have two, potentially interrelated functions:

1. As a scaffold for proteins of the exocytotic and endocytotic pathways, such as the exocyst and indirect effects through the actin cytoskeleton.[34–36]
2. As a lipid involved in the topological rearrangement of the plasma membrane during fusion and fission.

A distinguishing feature of PtdIns-4,5-P_2 is its high negative charge of ~ -4 at pH 7.[11] The highly charged lipid creates a highly dynamic electrostatic scaffold that interacts with unstructured (e.g., in MARCKS, GAP43) and structured (e.g., in PH and C2 domains) basic moieties on a variety of proteins (for a review see Ref. 12). Unstructured basic peptides cause lateral sequestration of PtdIns-4,5-P_2 on membranes *in vitro*

containing 1 mole% PtdIns-4,5-P_2 with as much as 30 mole % PS 13, an effect that is explained by electrostatic considerations.[14]

Several proteins that play important roles in exocytosis have structured basic moieties in C2 domains that interact with PtdIns-4,5-P_2 including synaptotagmin[15] and rabphilin.[16] Stop-flow techniques demonstrate that PtdIns-4,5-P_2 greatly speeds the Ca^{2+}-dependent interaction of synaptotagmin with membranes *in vitro*[17], suggesting that this interaction may have important physiological consequences. In addition, FRET has been used to show that PtdIns-4,5-P_2 directly interacts with syntaxin *in vitro*.[37] There are numerous proteins involved in exocytosis and endocytosis that contain a structured basic sequences in pleckstrin homology (PH) domains that interact with PtdIns-4,5-P_2. These include CAPS in the exocytosis pathway[19] and dynamin in the endocytosis pathway. PtdIns-4,5-P_2 also plays an important regulatory role in conjunction with small GTPases and proteins that regulate the actin cytoskeleton.[20] These pathways also influence fusion and fission.

While there is strong evidence for PtdIns-4,5-P_2 interacting with proteins that are important for fusion and fission, there is little direct evidence at this time for a direct role of the lipid in the fusion or fission reactions. For example, both long term and acute modulation of PtdIns-4,5-P_2 in chromaffin cells alter the size of the releasable granule pools but not the fusion kinetics,[21] consistent with a role prior to but not during fusion. Nevertheless, it seems likely that PtdIns-4,5-P_2 molecules with high charge and relatively high concentrations at fusion sites (as many as nine molecules in the cytoplasmic leaflet of the fusion pore) would directly influence lipid rearrangements. This is an important area for future investigation. It will be challenging to distinguish between the lipid simply being a scaffold for a multitude of proteins involved with trafficking at the plasma membrane, and having a direct function in the bilayer rearrangements of fusion and fission. In fact, these two roles may sometimes be indistinguishable, since one or more of the interacting proteins may have as its primary task the regulation of PtdIns-4,5-P_2 function in fusion or fission.

5.14.6 Biophysical Approaches to Understanding Viral Fusion Machines

The superficially shared structural features of HA with the SNARE proteins essential for internal cellular fusion have stimulated the hope that there is a universal mechanism for protein-mediated fusion. As the prototype of class I fusion proteins, and the epitope for flu serotyping the influenza virus HA has been studied extensively. While the speed of lipid mixing of HA-mediated fusion is rapid *in vitro* relative to infection speeds (**Figure 2**), fusion pore formation has not been measured and thus we do not know the kinetics of complete fusion for HA in an intact virus. However, the accessibility of HA-mediated cell-cell fusion, and the large body of investigation into HA make this the best studied fusion protein that is sufficient for fusion. We learn the importance of guided conformational transitions together with protein-protein interactions in conjunction with clear phenotypic discrimination between intermediates of hemifusion and the fusion pore opening and subsequent widening. Clearly there is much more work to be done, because we do not know why changing a single amino acid residue at the tip of the fusion peptide gives hemifusion instead of fusion.[38]

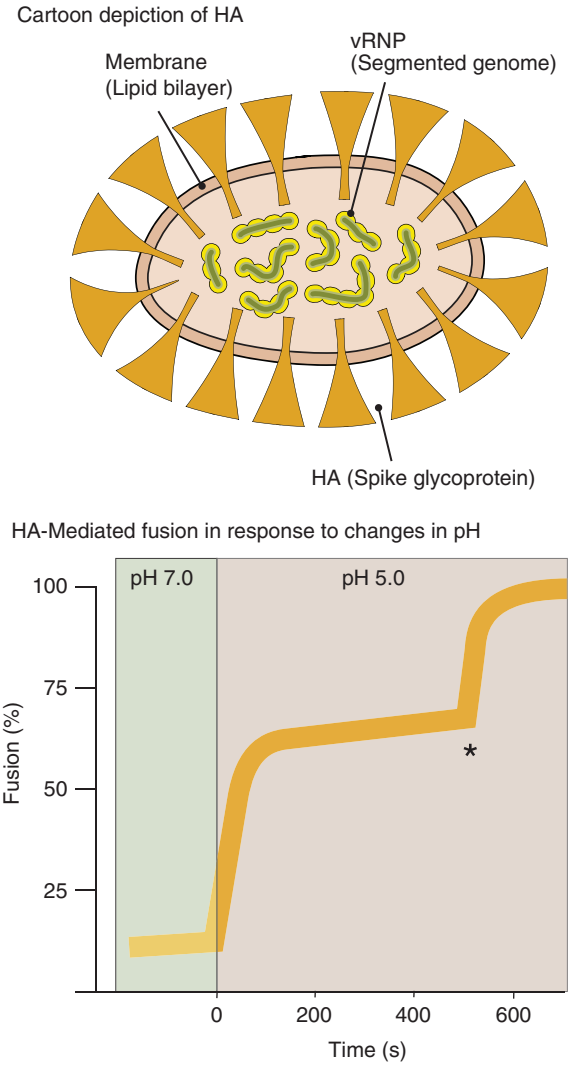

Figure 2 Cartoon depiction of HA virus particles and response of viral particle fusion *in vitro* to changes in pH. Viral particles were purified by sucrose-gradient centrifugation, labeled with octadecyl rhodamine (R18) at a concentration such that R18 fluorescence was quenched, and bound to the surface of liposomes at pH 7.0. Fusion of these viral particles bound to liposomes was triggered by rapid acidification to pH 5.0, with fusion measured by monitoring an increase in the emission at 590 nm due to dequenching of R18 upon lipid-mixing of the viral envelope and the lipid membrane. Triton X-100 (added at point of asterisk) induces complete dequenching of R18, and to calibrate the extent of fusion. Chu, V. C.; McElroy, L. J.; Chu, V.; Bauman, B. E.; and Whittaker, G. R. The avian coronavirus infectious bronchitis virus undergoes direct low-pH-dependent fusion activation during entry into host cells. *J. Virol.* **2006**, *80*(7), 3180–3188. Copyright by American Society for Microbiology.

HA is the first viral glycoprotein for which the structures of both pre- and post-fusion forms were solved at atomic resolution.[39,40] HA is synthesized as a single-chain precursor protein HA0, which then oligomerizes into a trimer during protein transport through the secretory pathway[41]. The precursor HA0 (549 amino acids in A/Hong Kong/68/H3N2) then needs to be cleaved into the HA1 and the HA2 polypeptides after the conserved arginine at residue 329 to be primed for the subsequent low pH-triggered conformational changes (**Figure 3**).[42]

Although the crystal structures of both pre- and post-fusion forms of HA have been available for more than a decade (**Figure 4**), we still do not know exactly how conformational rearrangements occur step by step, how low pH environment triggers the rearrangements of the HA ectodomain, and which structural elements are crucial for HA fusion activity.

It has been suggested that the low pH might lead to an enhanced protonation of the HA1 domain, and generate enough electrostatic repulsion force to partially dissociate the HA1 domain from the HA2 to allow the loop region in the HA2 to contact with water; this would cause the loop to transition into a helix and extend the pre-existing central coiled coil (**Figure 5**).[44–46] In this model, it seems that the only step requiring a low pH trigger is the exposure of the loop region connecting the two alpha helices in HA2 to water by partial disorientation of HA1 from HA2. Consistent with this idea, spontaneous formation of extended coiled coils are observed in bacterially expressed HA2 polypeptide at neutral pH, indicating that the low pH trigger is not necessary for the extension of coiled coils.[47] The prevailing hypothesis for the mechanism of how conformational changes lead to the fusion of two membranes is that extension of coiled coils triggered by the low pH directs the fusion peptide to insert into the target membrane, and then a helix-to-loop conformational change reorients the protein to pull the fusion peptide toward the transmembrane domain. These molecular transitions result in a tight packing of the COOH-terminus of HA2 against grooves of the NH_2-terminal coiled coil, proceeding to the fusion of the two bilayers.[48–50] This hypothesis emphasizes that both the extension of the coiled coil and the bending of the protein resulting from the helix-to-loop conformational change are important for fusion. The experimental results favoring this hypothesis demonstrate that a double proline substitution mutant (F63P/F70P) at the region supposedly undergoing loop-to-helix conformational change upon low pH failed to induce fusion, although the mutant still presented and inserted the fusion peptide to the target membrane.[50] The block to fusion was demonstrated to occur in the tight packing of

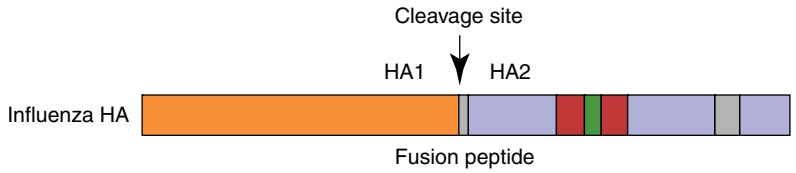

Figure 3 Cartoon depicting domain structure of HA. A single polypeptide is cleaved into polypeptides HA1 and HA2 (which reveals the fusion peptide) as indicated. HR1 and HR2 are the two heptad repeat regions of HA.

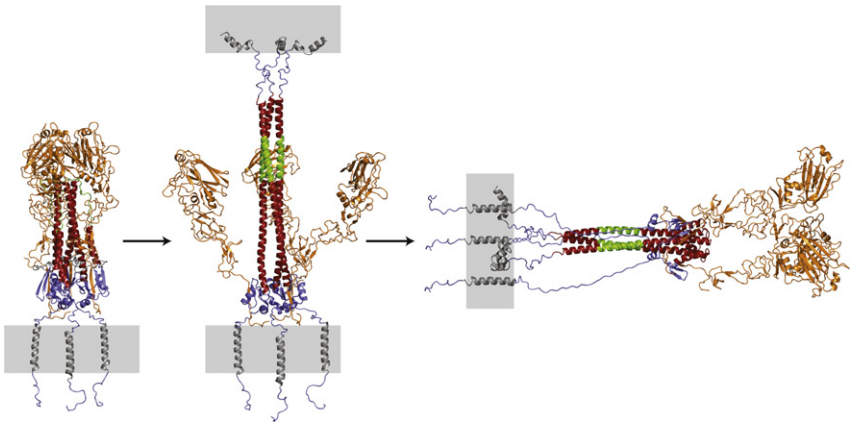

Figure 4 Cartoon depicting conformational stages during HA-mediated fusion. Regions of HA are colored according to **Figure 3**. Adapted from PDB 3HGM, 1HTM, 1IBN, 3HGM (Bullough, P. A.; Hughson, F. M.; Skehel, J. J.; Wiley, D. C. Structure of influenza haemagglutinin at the pH of membrane fusion. *Nature* **1994**, *371*, 37–43; Han, X.; Bushweller, J. H.; Cafiso, D. S.; Tamm, L. K. Membrane structure and fusion-triggering conformational change of the fusion domain from influenza hemagglutinin. *Nat. Struct. Biol.* **2001**, *8*, 715–720; Weis, W. I.; Brunger, A. T.; Skehel, J. J.; Wiley, D. C. Refinement of the influenza virus hemagglutinin by simulated annealing. *J. Mol. Biol.* **1990**, *212*, 737–761; Weis, W.; Brown, J. H.; Cusack, S.; Paulson, J. C.; Skehel, J. J.; Wiley, D. C. Structure of the influenza virus haemagglutinin complexed with its receptor, sialic acid. *Nature.* **1988**, *333*, 426–431. The regions modeled were created with a combination of manual modeling using the program Coot (Emsley, P.; Cowtan, K. Coot: model-building tools for molecular graphics. *Acta Crystallogr. D Biol. Crystallogr.* **2004**, *60*, 2126–2132). and PDB editing. These regions do not necessarily represent the actual conformation of the regions, but have the same number of residues of the protein and can visually illustrate how the virus protein functions.

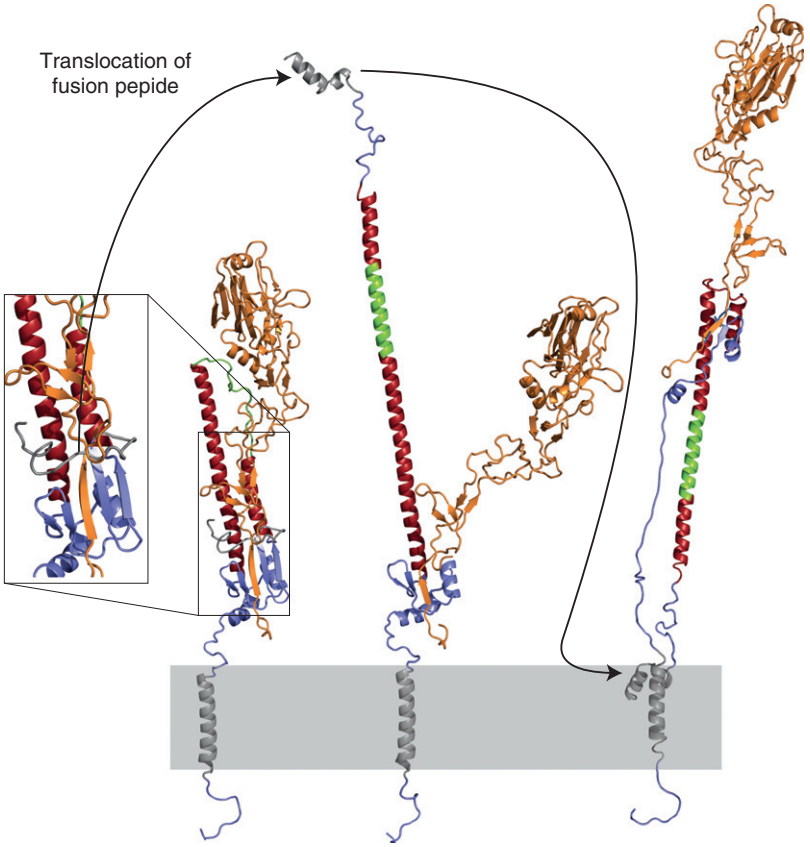

Figure 5 Cartoon depicting transitions of internal fusion peptide during HA-mediated fusion. Regions of HA are colored according to **Figure 3**. Adapted from PDB 3HGM, 1HTM, 1IBN, 3HGM (Bullough, P. A.; Hughson, F. M.; Skehel, J. J.; Wiley, D. C. Structure of influenza haemagglutinin at the pH of membrane fusion. *Nature* **1994**, *371*, 37–43; Han, X.; Bushweller, J. H.; Cafiso, D. S.; Tamm, L. K. Membrane structure and fusion-triggering conformational change of the fusion domain from influenza hemagglutinin. *Nat. Struct. Biol.* **2001**, *8*, 715–720; Weis, W. I.; Brunger, A. T.; Skehel, J. J.; Wiley, D. C. Refinement of the influenza virus hemagglutinin by simulated annealing. *J. Mol. Biol.* **1990**, *212*, 737–761, and Weis, W.; Brown, J. H.; Cusack, S.; Paulson, J. C.; Skehel, J. J.; Wiley, D. C. Structure of the influenza virus haemagglutinin complexed with its receptor, sialic acid. *Nature* **1988**, *333*, 426–431.) as described for **Figure 4**. For clarity, only one of the monomers of the trimer are depicted. Arrows point to the relative positions of the HA0 internal fusion peptide between the pre-fusion complex (left), the "docked" complex (middle, note that the target membrane is not shown), and the post-fusion complex (right).

COOH-terminal extended regions into the grooves between the helices of the NH_2-terminal half of the coiled coil due to the splayed NH_2-terminal half of HA2, suggesting that the insertion of fusion peptide into target membrane alone is not sufficient for fusion, and the tension caused by the packing of COOH-terminus against the NH_2-terminus of HA2 may be the driving force for membrane merging. Another piece of evidence for the role of the packing of the COOH-terminus to the NH_2-terminus in viral fusion is that the alanine substitution mutants at five apolar residues after the short COOH-terminus of HA2 fails to cause both lipid and content mixing.[51]

As a result of conformational changes of HA upon low pH exposure, the fusion peptide located at the tip of the HA2 molecule is exposed to the close proximity of the target membrane. When the target membrane is available, the fusion peptide inserts into the lipid bilayer to induce lipid mixing between the target cell membrane and the viral membrane. It has been experimentally determined that the free energy associated with the insertion of full-length fusion peptide into the lipid membrane is 4.5 kBT, and as many as 18 fusion peptides binding to the target membrane might generate enough energy to stabilize a stalk-like fusion intermediate, which has high membrane curvature.[52] While necessary for fusion, the packing of fusion peptides does not appear to be sufficient for fusion. Lipids present in the membrane act together with HA to cause fusion. Changing membrane lipid physical properties or composition in ways that well defined also blocks fusion, despite conformational-specific antibody binding indicating that HA is in the post-fusion state.[53] In other words the protein conformational change, while essential, is not sufficient, as there are post-protein conformational changes in lipid conformation that are needed for fusion to continue along its path. Thus the pathway of HA-mediated membrane fusion involves conformational changes to induce lipids to undergo the more general pathway outlined above for lipid membrane fusion.[53]

The role of the fusion peptide domain for HA-mediated membrane fusion has been the subject of many biophysical studies.[54] The fusion peptide of HA is rich in glycine; for example, influenza A/X31/H3N2 contains 6 glycine residues in 20 residues of fusion peptide (GLFGAIAGFIENGWEGMIDG). Extensive mutagenesis studies of fusion peptides have revealed

that both the primary sequence and the length of fusion peptide are crucial for HA fusogenic activity.[55] For example, HA2 G1E substitution abolishes cell-cell and RBC-cell fusion activity of expressed HA, while G4E substitution decreases fusion efficiency and elevated the pH threshold for activation.[56] Alanine can substitute for glycine at positions 1 and 4 without impacting HA-induced cell-cell fusion; however, the polar amino acid serine substitution for glycine at position 1 causes a hemifusion phenotype.[38] The requirements for specific amino acids at certain positions and for a defined length in the fusion peptide have been further supported by the NMR-solved structure of fusion peptide in detergent micelles and in model lipid membranes[43,52] stabilized by a charge-dipole interaction between the N-terminal Gly and the dipole moment of helix 2[54] (**Figure 6**). At acidic pH, the 20 residues of fusion peptide adopt a V-shaped 'boomerang' structure with an oblique NH_2-terminal amphipathic helix spanning residues 2–10 and a turn formed by residues 11, 12 and 13 followed by a short COOH-terminal helix[43,57] stabilized by a charge-dipole interaction between the N-terminal Gly and the dipole moment of helix 2[58] (**Figure 6**). The bent fusion peptide then may insert ~16–17 Å into the outer leaflet of the target membrane, almost to the mid-plane of the lipid bilayer with the residue Leu 2 and Phe 3 penetrating deepest into the membrane.[52,57] In the solution structure, the hemifusion phenotype mutant G1S has a similar structure to that of wild type, but the glycine ridge on the outer surface of the NH_2-terminal helical arm is disrupted. In contrast, the mutant G1V, where fusion is completely abolished, has a very irregular linear amphipathic helix instead of the fixed angled boomerang structure (**Figure 6**).[59,60] Another fusion-defective mutant, W14A, has a more flexible kink than that of the wild type, in contrast, the alanine substitution at phenylalanine residue 9 (F9A) has a similar structure to that of the wild-type and has no defect in fusion (**Figure 6**).[61] These studies suggest that both the angled and deeply inserted structure as well as the glycine ridge make a contribution to the fusion activity.

Despite the fact that we have gained a large amount of information on the structure of the influenza fusion peptide over the past several years, there are still open questions surrounding how the insertion of fusion peptide leads to fusion of viral membrane and target membrane and also with regard to the thermodynamic profile during the mixing of two bilayers. It has been generally accepted that the transmembrane domain (TMD) of HA2 and cooperation of multiple HA molecules are required in the fusion pore initiation and fusion pore enlargement.[62] Replacing the TMD of HA with a glycerylphosphatidylinositol (GPI) anchor or the deletion mutants with less than 17 residues in length cause a hemifusion phenotype, but a TMD with polar amino acids at the COOH-terminus still allows full fusion.[12,63] A synthetic peptide representing the transmembrane segment of X31/HA spans an artificial DMPC/DMPG bilayer as an α-helix that aligns roughly perpendicular to the bilayer membrane.

The consequences of HA fusion peptide insertion are not well understood, although it is clear that the proposed boomerang structure avoids placing the polar amino acids within the hydrophobic phase, which would be disruptive or structure-forming. Insertion of a charged amphipathic helix per se would tend to promote positive curvature, and might aid in "nippling" the membranes towards each other to contact prior to fusion, as in the proposed mechanism for synaptotagmin.[29]

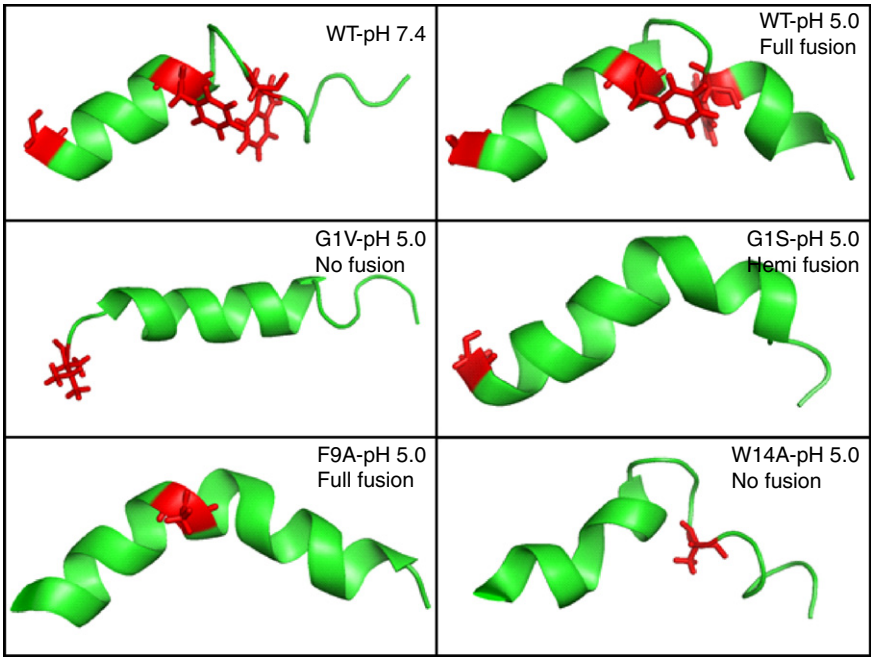

Figure 6 NMR structures of influenza virus HA fusion peptide and mutants in dodecylphosphocholine (DPC) micelles at pH 7.4 or pH 5.0. The structures of HA fusion peptides are shown in ribbon representation with the side chains of the mutated amino acids shown in stick representation (PDB accession numbers: WT-pH 7.4, 1ibo; WT-pH 5.0, 1ibn; G1V-pH 5.0, 1xop; G1S-pH 5.0, 1xoo, F9A-pH 5.0, 2jrd and W14A-pH 5.0, 2dci).

One suggestion is that the membrane helices of the fusion peptide and the TMD could interact with each other, so providing a driving force for the mixing of two membranes.[64] Other open questions include the study of HA fusion (and other enveloped viruses) in the context of negative membrane curvatures found in the multi-vesicular bodies of endosomal compartments,[65] and lipids known to be enriched in endosomes. Another open question is whether the HA conformational changes are strictly irreversible in the absence of a target membrane. The prevailing model that spring-loaded conformational changes are uni-directional is based in part on the fact that pre-treatment of virus particles from typical laboratory strains (e.g., the H3 strain X-31) with low pH effectively neutralizes infection. Analysis of other viral subtypes (e.g., H2) show features consistent with reversible conformational changes[66] and many natural isolates of influenza do not show the irreversible conformational changes associated with X-31 in the absence of a target membrane (G. Whittaker personal communication). Tatulian and Tamm[67] have demonstrated that the conformational change of the entire HA is reversible in the absence of bound target membranes.

The formation of a six-helix bundle (6HB) is the structural feature that characterizes class I viral fusion proteins. Because fusion peptides insert into target membranes and TMDs span the viral envelope, the folding of fusion proteins into hairpins brings the viral envelope and host cell membrane into proximity. Even for the two other classes of viral fusion proteins, which do not exhibit 6HBs and contain much β-sheet, in the final, post-fusion state, it is likely that fusion peptides and TMDs are proximal. It is not experimentally certain that this proximity occurs, because the hydrophobic TMDs and fusion peptides themselves are not present in the crystallized proteins. This apposition of the membrane imbedded TMD and fusion peptides of viral fusion proteins is similar to the proximity between TMDs of v- and t-SNAREs in their tetrameric coiled-coil. When the ubiquity of 6HBs was first demonstrated, it was assumed that bundle formation merely brought membranes into close contact, and fusion then occurred. We now know this is incorrect. The correlations between bundle formation and steps in the fusion process have been investigated for HIV-1 Env, Influenza HA, and ASLV Env. The precise steps of bundle formation depend on the precise protein. It appears that the longer the amino acid sequence that intervenes between TMDs and the coiled-coil, the earlier the bundle can form. For HIV-1 Env, which has a relatively short intervening sequence, not only does hemifusion occur prior to completion of bundle formation, but so does the creation of the initial fusion pore. Bundle formation releases considerable energy and the late occurrence of formation indicates that considerable energy is required for pore enlargement – the last step in fusion. In fact, several lines of evidence lead to the picture that hemifusion is energetically easy to achieve, pore formation more difficult, and pore enlargement even more difficult. From the theoretical point of view of membrane mechanics, considerable work must be expended to enlarge a fusion pore because additional membrane must be bent from its relaxed state as the pore enlarges.

The requirements for hemifusion are reasonably well understood: the standard Helfrich concepts of spontaneous membrane curvature and bending energy are sufficient to account for experimental observation. The mechanisms by which fusion proteins create the pore formation is less understood and how fusion proteins contribute to pore enlargement remains a mystery. For topological reasons, TMDs cannot span hemifusion diaphragms and can only enter the diaphragm from the junction between the diaphragm and the two original membranes. Common sense suggests that this entry of TMDs should destabilize the junction and thereby generate pores. This is consistent with demonstrations that TMDs are directly involved in pore formation[68] and with theory that predicts that pores form at the junction. But why TMDs are forced through the junction has not been addressed and the determinants of pore properties are virtually uncharacterized. For example, some viral fusion proteins, such as HIV-1 Env, generate large initial pores than readily open whereas others, such as influenza HA, create small pores that generally flicker open and closed before they enlarge. It seems reasonable that differences in pores are conferred by the proteins (rather than by the lipids), but the field has

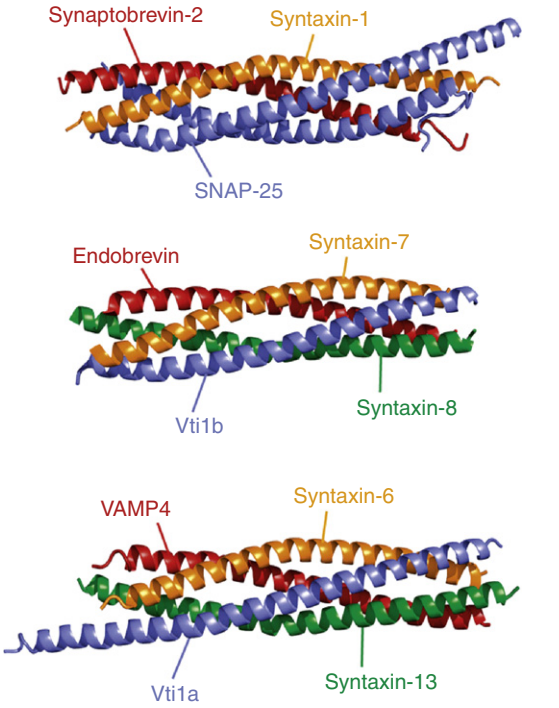

Figure 7 Core SNARE complex. Figure derived from references Sutton, R. B.; Fasshauer, D.; Jahn, R.; Brunger, A. T. Crystal structure of a SNARE complex involved in synaptic exocytosis at 2.4 A resolution. *Nature* **1998**, *395*, 347–353; Li, F.; Pincet, F.; Perez, E.; Eng, W. S.; Melia, T. J.; Rothman, J. E.; Tareste, D. Energetics and dynamics of SNAREpin folding across lipid bilayers. *Nat. Struct. Mol. Biol.* **2007**, *14*, 890–896; Antonin, W.; Fasshauer, D.; Becker, S.; Jahn, R.; Schneider, T. R. Crystal structure of the endosomal SNARE complex reveals common structural principles of all SNAREs. *Nat. Struct. Biol.* **2002**, *9*, 107–111; and Zwilling, D.; Cypionka, A.; Pohl, W. H.; Fasshauer, D.; Walla, P. J.; Wahl, M. C.; Jahn, R. Early endosomal SNAREs form a structurally conserved SNARE complex and fuse liposomes with multiple topologies. *EMBO. J.* **2007**, *26*, 9–18. It shows the core SNARE complex formed by the three SNARE proteins involved in synaptic vesicle exocytosis, and the four SNARE proteins involved in late and early endosomal function in mammalian and yeast cells respectively.

not formulated guiding principles as to which structural features of a protein control pore properties. Because viral nucleocapsids can only enter cytosol if a pore enlarges, these questions are potentially of practical, in addition to biophysical, importance.

The SNARE complex formed between two fusing membranes are the principal fusogens of the eukaryotic molecular machinery that mediates membrane fusion in intracellular trafficking pathways.[69] The SNARE complex is a coiled bundle of four parallel helices provided by three or four individual SNARE protein molecules (Figure 7). Perhaps the best studied is the SNARE complex mediating neuronal exocytosis containing four helices provided by three SNARE proteins: SNAP-25 (synaptosome-associated protein of 25 kD), synaptobrevin-2, and syntaxin-1.[70] The free energy generated during the assembly of a single ternary SNARE is estimated to be 20–35 k_BT.[71–73] A key question is what proportion of the energy of SNARE complex formation is directed at membrane fusion and what the contribution of the energetics of this reaction, if any, contribute to membrane docking and tethering.

5.14.7 Questions Arising from Structural Studies of SNARE Proteins

Several of the proteins engaged in and/or responsible for fusion have been studied at atomic resolution with biophysical structural approaches. These studies have greatly illuminated our understanding of the protein machines driving membrane fusion reviewed in Refs. 75 and 76. The minimal domains of SNARE proteins that can spontaneously engage in a stable 4-helix SNARE complex revealed a characteristic packing at the core of the SNARE complex. The majority of the packing interactions are hydrophobic, however there is an ionic layer typically consisting of a single arginine and three glutamine residues.[70,74] This ionic layer is found at the midpoint of the coiled-coiled bundle and hence is referred to as the zero ionic layer. The zero ionic layer is an evolutionarily conserved feature of all SNARE complexes examined to date, however the functional role of this feature is not known. Biophysical characterization of SNARE complexes that perturb the zero ionic layer suggest that it may be important for the stability of SNARE complexes.[77] One idea was that this layer could provide an intervention point for SNARE complex disassembly, however perturbation of the layer in an *in vitro* disassembly assay[78] had no discernable impact on NSF/SNAP catalyzed SNARE disassembly. Current hypotheses for how polar zero layer residues might impact SNARE function favor potential role(s) in SNARE complex assembly, such as the suggestion that a polar zero layer helps align assembly of the SNARE helices in register, or in other downstream functions of the SNARE complex. Mutagenesis studies of the zero ionic layer in different systems suggest different effects, but they are all relatively subtle.[79,80] Clearly, the influence of particular residues may vary according to the individual SNARE complex in question and the local parameters governing the assembly of a particular cognate SNARE complex.

Structures of the individual SNARE proteins have been tremendously stimulating in posing novel questions. The coiled-coil α-helix of synaptobrevin extends to the most membrane proximal residue, lysine[87] and this residue is also part of the extended transmembrane helix. The energetics and topology of SNARE complex formation may influence local bending of the α-helix at the interfacial region, which in turn could generate local membrane destabilization to aid fusion (Figure 8). It is not known how the membrane itself may locally influence the structure of cytoplasmic portions of synpatobrevin or other proteins involved in fusion. A recent structure of lipid-bound synpatobrevin suggests that the amphipathic helix 1 of synpatobrevin may lie on the surface of the membrane,[81] providing a molecular explanation of the observation that the membrane may influence the cytoplasmic portion of synaptobrevin to adopt conformations not observed in the absence of lipid.[82]

Some SNAREs contain independently folded NH_2-terminal domains together with additional unstructured linker regions of significant length. The presence of such domains and their ability to interact inter- and intra-molecularly significantly increases the complexity of SNARE complex formation and the ability of the SNARE proteins to drive membrane fusion. Syntaxin contains a linker region connecting the SNARE domain with the H_{ABC} NH_2-terminal domain. Fully extended, this region may be up to approximately 120 Å in length (Figure 9). It is currently unknown whether there are proteins that selectively bind to or regulate this region. In contrast to synaptobrevin, syntaxin has an slightly extended membrane proximal region that may not be part of the initial core SNARE complex structure (residues 260–265). The post-fusion SNARE complex shows this region adopts an α-helical structure that directly links the SNARE complex α-helix to the transmembrane α-helix. The local secondary structure adopted by these residues prior to fusion is unknown; secondary structural predictions suggest the region is unstructured and could conceivably act as a hinge facilitating the molecule to sample up to a 290 Å radius of the membrane proximal area (Figure 10).

There is evidence for an initial NH_2-terminal interaction between the SNARE proteins, but the final low energy 4-helical bundle may not be an intermediate in fusion, but rather either a dead-end conformation or a post-fusion conformation. An experiment missing from the field is a demonstration of helical bundle formation before, or simultaneous with fusion pore formation, as described above for viral fusion. There is strong evidence that prior interaction between the plasma membrane SNAREs syntaxin and SNAP25 increases rate of interaction with VAMP.[83]

The relationship of the post-fusion SNARE complex (Figure 11) to lipid rearrangements that occur during fusion and content mixing are currently not known. One study has placed syntaxin as a pore-forming molecule with 5–8 syntaxin molecules making up a fusion pore.[84] Assembly of 5–8 SNARE complexes as a minimum number required to drive fusion events is in good agreement with theoretical considerations of the energetics of SNARE complex assembly and membrane fusion. ~8 SNARE complexes were required to promote fast fusion in supported bilayer experiments,[85] and fewer in other lipid mixtures including PE, presumably because PE promotes fusion by curvature.[86] What is enormously fascinating is how the protein fusogens form such a pore, how the pore forms initially and how the pore dilates as fusion proceeds to completion. These pathways may have different kinetic and

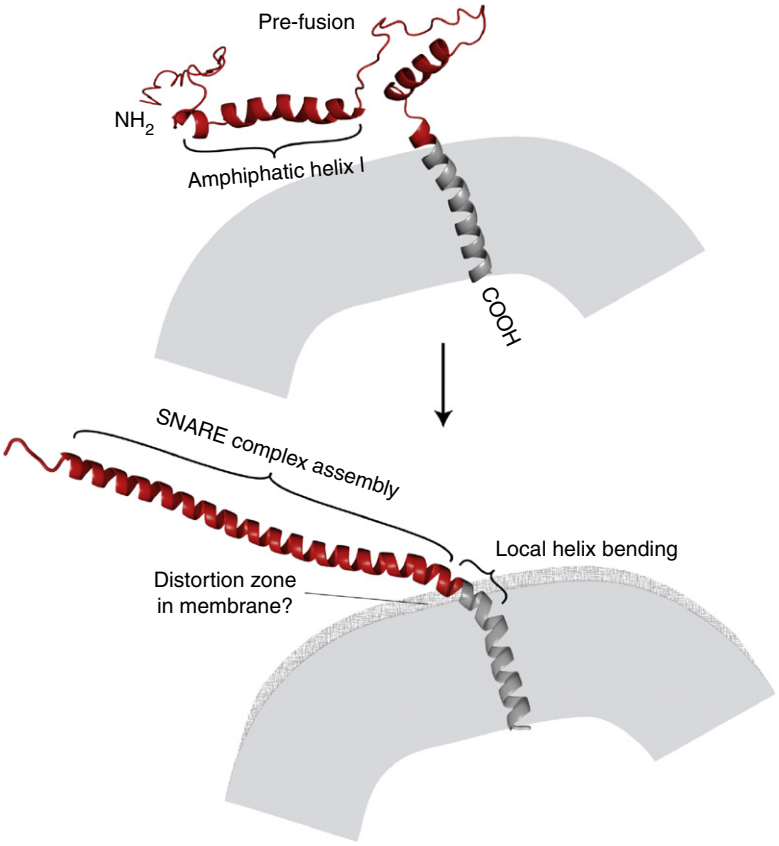

Figure 8 Structures of synaptobrevin in pre- and post-fusion conformations. Reproduced from Sutton, R. B.; Fasshauer, D.; Jahn, R.; Brunger, A. T. Crystal structure of a SNARE complex involved in synaptic exocytosis at 2.4 A resolution. *Nature* **1998**, *395*, 347–353 and Ellena, J. F.; Liang, B.; Wiktor, M.; Stein, A.; Cafiso, D. S.; Jahn, R.; Tamm, L. K. Dynamic structure of lipid-bound synaptobrevin suggests a nucleation-propagation mechanism for trans-SNARE complex formation. *Proc. Natl. Acad. Sci. U. S. A.* **2009**, *106*, 20306–20311 showing the structure of free and SNARE-complex engaged synaptobrevin. The extended membrane anchor has been modeled into the post-fusion structure and suggests a continuous α-helix from the membrane into the coiled-coil helix of the SNARE complex. Engagement of synaptobrevin with the parallel helices of the SNARE molecules may influence local bending of the helix at the membrane interface and could result in membrane compression.

thermodynamic parameters for different types of biological fusion, depending on the physiological requirements of the particular fusion event. The SNARE machinery certainly appears to have the potential for adaptability, mediating types of fusion as diverse as "kiss and run", complete fusion during constitutive events of exocytosis and homotypic fusion events such as those between endosomes.[87]

The SNARE complexes for which the structures have been solved all contain the four helix bundle in a parallel orientation. Perhaps not surprisingly, given the versatility of coiled-coil structures, the SNARE domains are also capable of associating in anti-parallel bundles, which are also stable, although not as stable as the parallel bundles.[88] This is superficially reminiscent of the anti-parallel and parallel coiled-coil transitions experienced by different conformations of HA (**Figures 4** and **5**) although caution should be exercised in extending these analogies given the topological constraints of the fusion machinery.

It is not known what such associations may represent physiologically; they could possibly represent a means of tethering membranes independently of fusion, or may be unproductive molecules requiring reconditioning by accessory factors in order to participate in multiple rounds of membrane fusion.

The profile of the energy landscape[89] traversed by the fusion reaction will be influenced by a multitude of exogenous factors. Known factors include the membrane lipid composition, the availability of SNARE proteins in suitable pre-fusion states and the specific activity of SNARE accessory factors (**Table 1**). These factors can have multiple influences, for example, membrane composition can play a role in providing molecular determinants for protein assembly and will also determine membrane elasticity. How conformational changes amongst SNARE proteins and their accessory factors control the thermodynamics and kinetics of docking, lipid mixing and content mixing after membrane fusion remain open questions.

5.14.8 Single Molecule Studies of Membrane Fusion

Our understanding of the conformational plasticity of protein machineries and the hysteresis properties of biological fusion machines lead to an appreciation for the energetic complexities of the fusion reaction. The use of single molecule studies to unravel the complex energy landscape of membrane fusion will be an important biophysical approach with tremendous potential to relate the topography of the energy landscape to

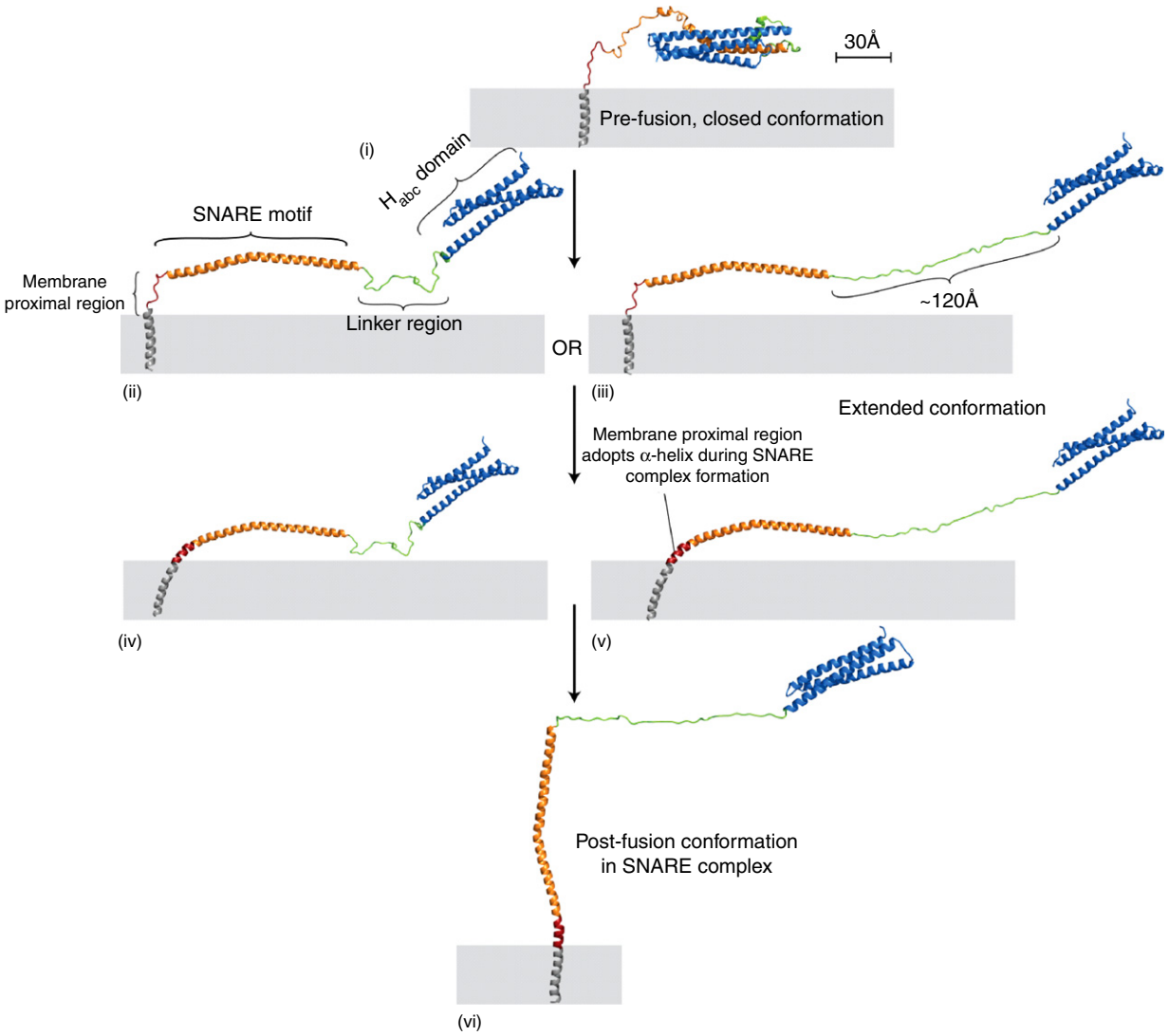

Figure 9 Cartoon depicting conformational changes of syntaxin before, during and after fusion. Syntaxin protein models adapted from PDB 3C98, 3IPD, 1BR0, 1SFC (Sutton, R. B.; Fasshauer, D.; Jahn, R.; Brunger, A. T. Crystal structure of a SNARE complex involved in synaptic exocytosis at 2.4 A resolution. *Nature* **1998**, *395*, 347–353; Burkhardt, P.; Hattendorf, D. A.; Weis, W. I.; Fasshauer, D. Munc18a controls SNARE assembly through its interaction with the syntaxin N-peptide. *Embo. J.* **2008**, *27*, 923–933; Stein, A.; Weber, G.; Wahl, M. C.; Jahn, R. Helical extension of the neuronal SNARE complex into the membrane. *Nature* **2009**, *460*, 525–528; and Fernandez, I.; Ubach, J.; Dulubova, I.; Zhang, X.; Sudhof, T. C.; Rizo, J. Three-dimensional structure of an evolutionarily conserved N-terminal domain of syntaxin 1A. *Cell* **1998**, *94*, 841–849.) illustrating various possible conformations sampled by syntaxin between the pre-fusion and post-fusion complexes. Of particular interest during these conformational changes en route to fusion is the role of the membrane proximal region in extending the SNARE domain (red) and the extended linker (green) between the SNARE domain (yellow) and the H_{ABC} domain (blue).

the mechanism and regulation of fusion. Although the application of this approach to studying biological fusion machines is relatively new,[72,125–130] such experiments have some additional advantages – such as being able to distinguish fusion events from vesicle aggregation or vesicle rupture. Single molecule approaches of fluorescently-labeled virus in living cells has allowed visualization of influenza fusion with intracellular compartments/endosomes,[131] and the use of solid supported lipid bilayers,[132] facilitates a more detailed analysis of the single-particle kinetics of HA-mediated fusion as well as SNARE-mediated fusion.[85] In combination with assays that reflect lipid and content mixing, together with pore formation and expansion, such approaches are expected to contribute substantially towards providing missing information regarding the intermediates and pathways involved in fusion.

5.14.9 What Can Membrane Fission Tell Us About Membrane Fusion?

Recent work has shown that two rungs of a dynamin spiral is the minimal structural unit responsible for the formation of the fission neck and hemifission intermediate in model membrane nanotubes (**Figure 12**).[133,134] Neck transformation

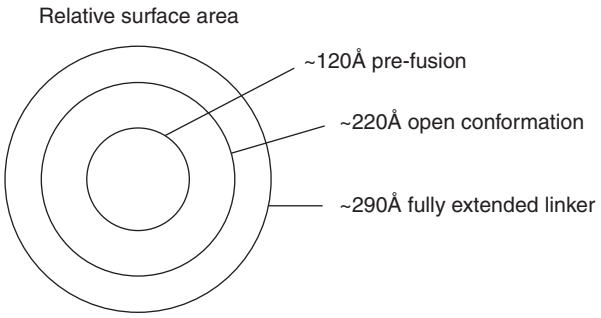

Figure 10 Relative membrane surface area potentially sampled by different syntaxin conformations. Schematic demonstrating the potential span of syntaxin at various stage of SNARE complex assembly from the pre-fusion, closed conformation (**Figure 9(i)**) to its conformation in the post-fusion SNARE complex (**Figure 9(vi)**).

requires the same hemifusion event, but in a cylindrically symmetrical way, as the inner leaflet of the tube must touch itself in the center to allow for the hemifission intermediate. Once again, it is relatively straightforward to calculate the ring conditions that will lead to constriction and narrowing of the tube towards the center, as long as the distance between the two rings is not too short. But once again, we are faced with the hydration force resisting any further constriction of the neck, since the surfaces of the inner leaflet lipids would have to come closer than the 2 nm equilibrium distance between attractive dispersion forces and repulsive hydration forces. But lo, there is a new modality for minimizing energy in this system; it is the tilt-like movement of lipid head groups away from each other at the very center of the hourglass constriction of the neck (**Figure 12(a)**, third panel). This tilting of the lipids at the center of the inner monolayer of the neck results

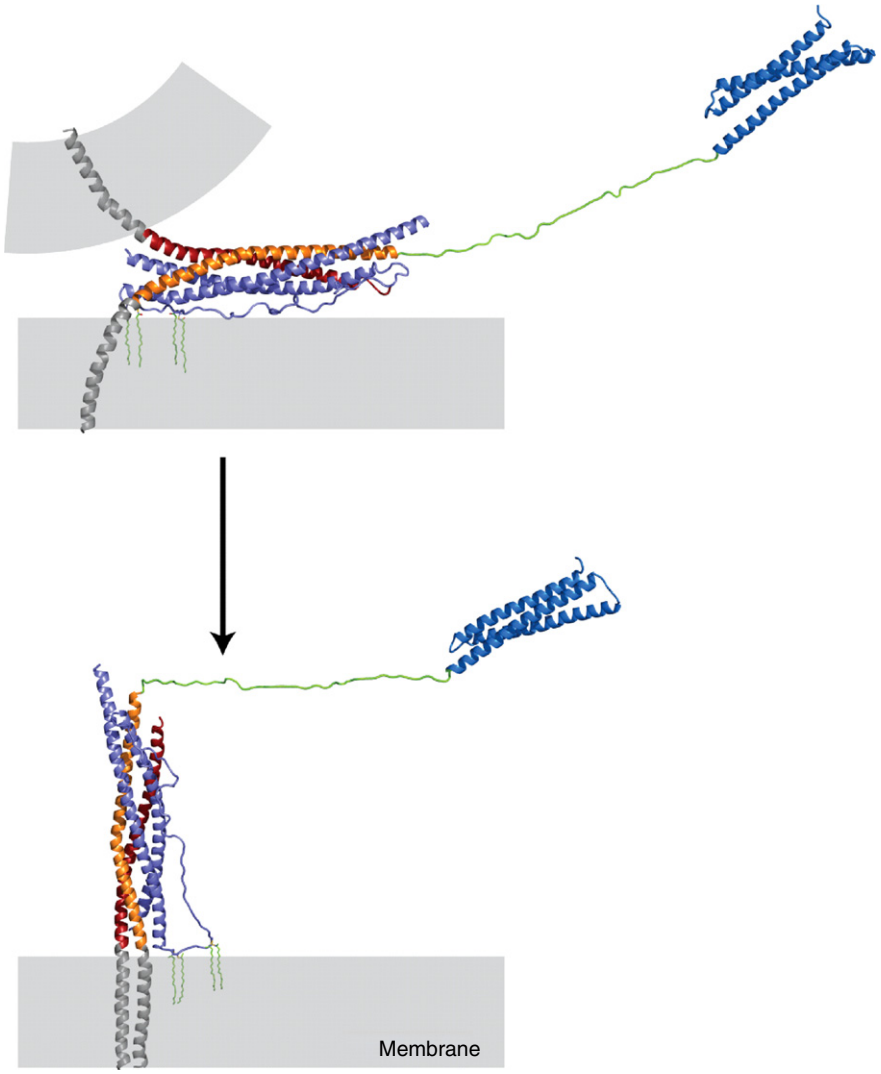

Figure 11 Neuronal SNARE complex assembling in transit to fusion. Reproduced from Sutton, R. B.; Fasshauer, D.; Jahn, R. Brunger, A. T. Crystal structure of a SNARE complex involved in synaptic exocytosis at 2.4 A resolution. *Nature* **1998**, *395*, 347–353; Antonin, W.; Fasshauer, D.; Becker, S.; Jahn, R.; Schneider, T. R. Crystal structure of the endosomal SNARE complex reveals common structural principles of all SNAREs. *Nat. Struct. Biol.* **2002**, *9*, 107–111; and Zwilling, D.; Cypionka, A.; Pohl, W. H.; Fasshauer, D.; Walla, P. J.; Wahl, M. C.; Jahn, R. Early endosomal SNAREs form a structurally conserved SNARE complex and fuse liposomes with multiple topologies. *EMBO. J.* **2007**, *26*, 9–18. It shows two states of the parallel SNARE complex in *cis* during directed SNARE complex assembly and in *trans* in the post-fusion conformation. The four sites of palmitoylation of SNAP-25 are indicated.

Table 1 Proteinaceous SNARE accessory factors (physiological and non-physiological)

Factor	*Comment(s)*	*Reference*
Clostridial neurotoxins (CNTs)	tetanus toxin (TeNT) and botulism toxin (BoNT) 7 serotypes (A-G) function through proteolytic cleavage of one of the SNARE complex proteins required for synaptic vesicle fusion. Zinc metalloproteases with very specific target selectivity.	(90,91)
Complexin	Complexins possess a central α helix that binds in an antiparallel fashion to a groove in the central part of the helical SNARE bundle, formed by syntaxin 1 and synaptobrevin.	(92,93)
Cysteine string protein	Member of the DNAJ family of chaperones, mouse knockout results in neurodegeneration.	(79,94)
DDI1/VSM1	Protein contains both a ubiquitin-interacting UBA domain and a ubiquitin-like UBL domain.	(95,96)
DSL1	Part of a tethering complex involved in COPI vesicle trafficking.	(97)
EEA1	Binds H_{ABC} domain of Syntaxin 6	(98)
GATE-16	Ub-fold protein, *S. cerevisiae* ortholog, Atg8 functions in autophagy.	(99,100)
IncA, IcmG/DotF	Bacterial effector proteins with inhibitory SNARE function employed by pathogens to manipulate host cell trafficking.	(101)
Munc-13	Contains a conserved DAG binding C1 domain.	(102–105)
NSF/Sec18	Member of the AAA ATPase protein chaperone family	(106)
PRA3/YIP1	Integral membrane protein capable of interaction with the lipid-moiety of prenylated proteins and the TM domain of SNAREs.	(87,107)
Rabphilin	Rab3 effector containing C2 domains	(108)
SHIP164	Paralog UHRF1BP1	(109)
SM proteins	nsec-1/Munc18-1 binds to syntaxin-1 with nM affinity; Sec1p is essential for exocytosis in yeast.	(110–112)
SRO7/tomosyn	Syntaxin1a binding protein and Rab GTPase effector with WD40 repeat motifs, also related to lethal giant larvae.	(113–115)
α-SNAP	Acts in partnership with NSF in SNARE disassembly.	(116,117)
Synaptotagmin	Contain single transmembrane domain and two membrane-distal C2 domains (C2A and B), which act as specialized domains to induce membrane stress in response to Ca^{2+}. Other C2 domain proteins such as Doc2b, may function similarly.	(10,29,118–120)
Synaptophysin	Integral membrane protein of synpatic vesicles present in higher eukaryotes.	(121,122)
α-synuclein	Ectopic expression can reverse the otherwise lethal neurodegeneration of cysteine string protein-α knockout mice.	(123,124)

in formation of a narrow separation of heads exposing the hydrophobic interior of the bilayers, termed a hydrophobic "belt" to indicate its presence as a ring (you can visualize this ring by rotating the figures of **Figure 12(a)** around the axis of the horizontal dashed line under each bilayers). Now the repulsive hydration force stabilizing inner aqueous diameters of 2 nm gives way to a newly developed hydrophobic attractive force, which is effectively the desire of water to desolvate the space between the tilting headgroups in the center. This water ejection leads to the close approximation and finally merger of the neck with itself at the midpoint; that is, its closure.

Figure 12(d) shows the calculated energy of a 9-mm-long segment of neck, depending upon the width (H) and radius (Rmid) of the hydrophobic belt discussed above. Like the stalk, the belt width becomes that of a single monolayer at the point of merger. The energy barrier of 35 k_BT is also similar to those calculated for membrane fusion,[24] so it is energetically feasible. The lipid bending and tilting needed to catalyze membrane merger are mainly motivated by high curvature stress in the neck inner leaflet. Accordingly, the energy barrier depends sharply on the minimal radius of the thinned neck, Rmin, which should approach 1–2 nm for the fission to occur, as seen in other estimations of hemifission.[135]

Thus the rings of protein acting on the outside of a 12 nm tube lead to boundary conditions whose effects propagate through the bilayer to influence and stress lipids facing each other across water, leading to their head groups parting and their oils merging in energetically feasible hemifission. The proteins act at length scales consistent with what we know about protein structural lengths, and the lipids respond fluidly to the protein's influence.

Mechanistic studies concerning dynamin offer not only a static view of the energetics of non-leaky fission/fusion reactions but also insights into the dynamics of the transition structures. Dynamin assembly shapes bilayers into highly curved structures (**Figure 12**). Assembly also greatly enhances the rate of GTP hydrolysis (100-fold),[136] which in turn leads to dynamin disassembly. Thus, assembly is self-limited in the presence of GTP. Recent experiments suggest that assembly-induced GTPase activity reduces the interaction of dynamin with the highly curved lipid membrane even before disassembly.[137] The result is the unstable, highly curved lipid neck described above that resolves either in membrane fission (endocytosis, described above), or reversal of high membrane curvature. From these studies, performed in model membranes, membrane fission may therefore be considered to be a *stochastic* result of GTP hydrolysis.[133,139] Studies in adrenal chromaffin cells suggest that

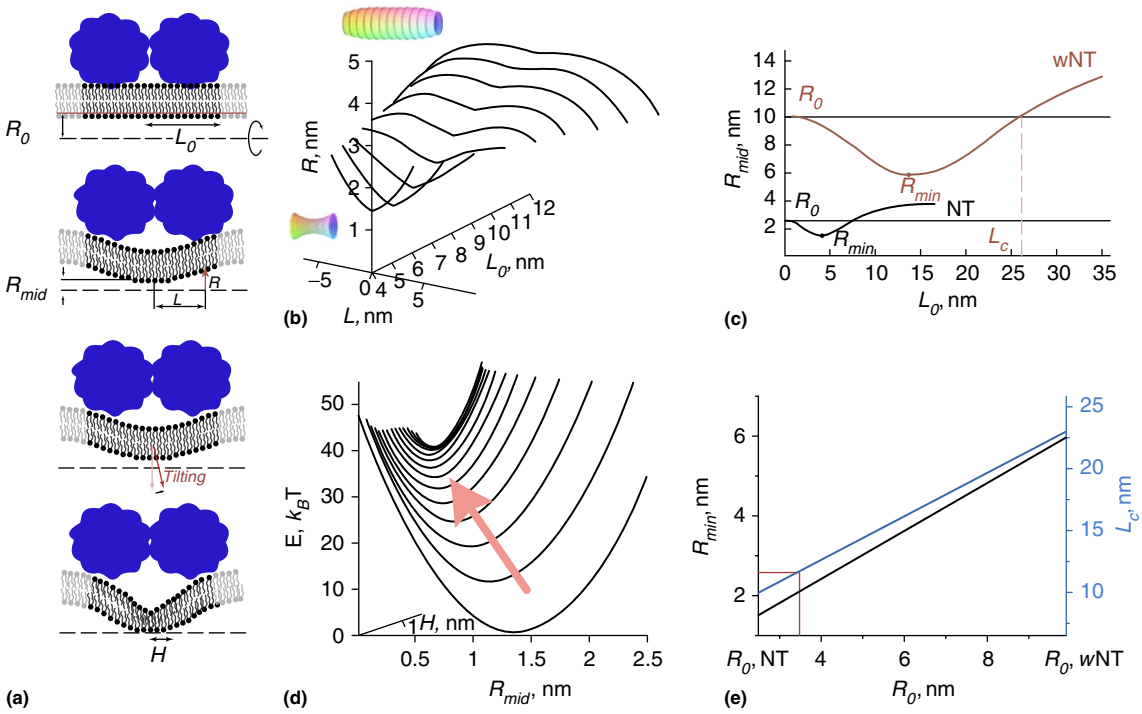

Figure 12 Theoretical analysis of local membrane rearrangements by Dynamin. (a) The pathway of membrane rearrangement leading to the fission of a short membrane neck detached from a dynamin scaffold (blue) upon GTP hydrolysis; the upper half of the neck membrane is shown. The neck constriction is followed by rearrangement of the thinnest part of the neck: lipids, by synchronous tilting, expose a small part of the hydrophobic membrane interior (hydrophobic belt). If the radius of the neck at the midpoint (R_{mid}) is small enough, expansion of the belt correlated with thinning of the neck becomes possible, and the neck closes completely. The neutral surface 140 of the inner monolayer of the neck membrane is shown by the red line. The function $R(L)$ describes the shape of this surface in the coordinate system (R, L); the coordinate center is placed in the midst of the neck (where Rmid is measured), so that the total length of the detached neck is $2L_0$. This length and the radius of the neck at both ends (R_0) are fixed by the dynamin scaffold (note that R_0 equals the radius of the nanotube in the dynamin-squeezed state and is about 0.5 nm bigger than the luminal radius, R_L). (b) Calculated shapes of necks ($R(L)$) detached from the dynamin scaffold of different initial length (L_0). Necks shorter than a critical length L_c (see [c]) narrow ($R_{mid} < R_0$), whereas longer necks bulge; calculated 3D shapes of shortest and longest necks are shown. (c) Numerically calculated dependence of the Rmid of the neck length L_0 for NT and wNT. From this dependence, the minimal radius of the neck (R_{min}) and the critical length L_c (at which $R_{mid} = R_0$) are determined. (d) Energy diagram showing the dependence of free energy of the neck ($R_0 = 2$ nm) upon the width (H) and the radius (R_{mid}) of the hydrophobic belt. The energy barrier along the pathway indicated by the red arrow is $\sim 35\ k_BT$. (e) Dependence of the critical length, L_c, (blue) and the neck radius in the narrowest place, R_{min}, (black) on R_0. Reproduced from Bashkirov, P. V.; Akimov, S. A.; Evseev, A. I.; Schmid, S. L.; Zimmerberg, J.; Frolov, V. A. GTPase cycle of dynamin is coupled to membrane squeeze and release, leading to spontaneous fission. *Cell* **2008**, *135*, 1276–1286.

dynamin functions in a similar way to control the fate of a recently fused secretory granule. Increasing the dynamin GTPase activity increases the rate of fusion pore expansion and the likelihood of rapid endocytosis.[138] The results are consistent with a function for dynamin in restricting fusion pore expansion. Increased GTP activity catalyzes a more rapid stochastic decision that results in either fusion pore expansion or (less frequently) membrane fission and endocytosis.

5.14.10 Perspective

Recent theoretical and experimental studies of membrane fission by dynamin and viral matrix protein reveal how protein complexes are arranged to effectively apply localized curvature stress to membranes without perturbing lateral membrane integrity; that is, without leakage. One conceptual approach is that sites of membrane remodeling are organized as membrane domains, both through membrane composition and membrane curvature; thus membrane remodeling is a collaborative effort accomplished by the entire domain, involving protein complexes and multiple lipids. We emphasize that despite decades of studies we still know only a little about fundamental physical principles underlying the spatial and temporal organization of membrane domains specialized in membrane remodeling. For example, the structure and composition of the fusion pore are unknown. New synergistic experimental and theoretical approaches are needed to resolve how proteins merge and separate membranes. For example, the ability to detect submicron deformations of the plasma membrane with the combination of polarization and TIRFM techniques[138,139] permits detection of the expanding fusion pore and may enable investigations of the molecular basis for membrane curvature changes in living cells.

The key is to study membrane remodeling in the context of concrete biological processes, taking into account corresponding length scales for the key membrane intermediates, dynamic cooperation between protein machineries and lipids,

component segregation and sorting and, importantly, long-range interactions which are, ultimately, of critical importance for highly localized membrane rearrangements leading to membrane fusion or fission.

Acknowledgments

This work was supported by NIH Grant no. 5R01GM069596 to R. Collins, R56-NS38129 to RWH, and the Intramural Program of the NICHD, NIH. Many thanks to Fabio Rinaldi for help with figure preparation, Fred Cohen for his discussion of the viral helical bundle timing experiments, and Gary Whittaker for helpful discussions.

References

[1] Gong, Y.; Ma, M.; Luo, Y.; Bong, D. Functional determinants of a synthetic vesicle fusion system. *J. Am. Chem. Soc.* **2008**, *130*, 6196–6205.
[2] Haque, M. E.; McIntosh, T. J.; Lentz, B. R. Influence of lipid composition on physical properties and peg-mediated fusion of curved and uncurved model membrane vesicles: "nature's own" fusogenic lipid bilayer. *Biochemistry* **2001**, *40*, 4340–4348.
[3] Jackson, M. B.; Chapman, E. R. Fusion pores and fusion machines in Ca^{2+}-triggered exocytosis. *Annu. Rev. Biophys. Biomol. Struct.* **2006**, *35*, 135–160.
[4] Hoppins, S.; Nunnari, J. The molecular mechanism of mitochondrial fusion. *Biochim. Biophys. Acta.* **2009**, *1793*, 20–26.
[5] Chan, D. C. Mitochondrial fusion and fission in mammals. *Annu. Rev. Cell. Dev. Biol.* **2006**, *22*, 79–99.
[6] Kozlov, M. M.; McMahon, H. T.; Chernomordik, L. V. Protein-driven membrane stresses in fusion and fission. *Trends Biochem. Sci.* **2010**, *35*(12), 699–706.
[7] Chernomordik, L. V.; Kozlov, M. M. Protein-lipid interplay in fusion and fission of biological membranes. *Annu. Rev. Biochem.* **2003**, *72*, 175–207.
[8] Martens, S.; McMahon, H. T. Mechanisms of membrane fusion: disparate players and common principles. *Nat. Rev. Mol. Cell. Biol.* **2008**, *9*, 543–556.
[9] Sorensen, J. B. Conflicting views on the membrane fusion machinery and the fusion pore. *Annu. Rev. Cell. Dev. Biol.* **2009**, *25*, 513–537.
[10] Chapman, E. R. How does synaptotagmin trigger neurotransmitter release? *Annu. Rev. Biochem.* **2008**, *77*, 615–641.
[11] Chanturiya, A.; Chernomordik, L. V.; Zimmerberg, J. Flickering fusion pores comparable with initial exocytotic pores occur in protein-free phospholipid bilayers. *J. Proc. Natl. Acad. Sci. U. S. A.* **1997**, *94*, 14423–14428.
[12] Melikyan, G. B.; White, J. M.; Cohen, F. S. GPI-anchored influenza hemagglutinin induces hemifusion to both red blood cell and planar bilayer membranes. *J. Cell. Biol.* **1995**, *131*, 679–691.
[13] Chernomordik, L. V.; Frolov, V. A.; Leikina, E.; Bronk, P.; Zimmerberg, J. The pathway of membrane fusion catalyzed by influenza hemagglutinin: restriction of lipids, hemifusion, and lipidic fusion pore formation. *J. Cell. Biol.* **1998**, *140*, 1369–1382.
[14] Kozlov, M. M.; Markin, V. S. Possible mechanism of membrane fusion. *Biofizika* **1983**, *28*, 242–247.
[15] Ginsberg, L.; Gershfeld, N. L. Phospholipid surface bilayers at the air-water interface. II. Water permeability of dimyristoylphosphatidylcholine surface bilayers. *Biophys. J.* **1985**, *47*, 211–215.
[16] Markin, V. S.; Kozlov, M. M.; Borovjagin, V. L. On the theory of membrane fusion. The stalk mechanism. *Gen. Physiol. Biophys.* **1984**, *3*, 361–377.
[17] Neher, E. Asymmetric membranes resulting from the fusion of two black lipid bilayers. *Biochim. Biophys. Acta.* **1974**, *373*, 327–336.
[18] Chanturiya, A.; Leikina, E.; Zimmerberg, J.; Chernomordik, L. V. Short-chain alcohols promote an early stage of membrane hemifusion. *Biophys. J.* **1999**, *77*, 2035–2045.
[19] Chizmadzhev, Y. A. The mechanisms of lipid-protein rearrangements during viral infection. *Bioelectrochemistry.* **2004**, *63*, 129–136.
[20] Zimmerberg, J.; Kozlov, M. M. How proteins produce cellular membrane curvature. *Nat. Rev. Mol. Cell. Biol.* **2006**, *7*, 9–19.
[21] Chernomordik, L.; Kozlov, M. M.; Zimmerberg, J. Lipids in biological membrane fusion. *J. Membr. Biol.* **1995**, *146*, 1–14.
[22] Helfrich, W.; Prost, J. Intrinsic bending force in anisotropic membranes made of chiral molecules. *Phys. Rev. A.* **1988**, *38*, 3065–3068.
[23] Cohen, F. S.; Akabas, M. H.; Zimmerberg, J.; Finkelstein, A. Parameters affecting the fusion of unilamellar phospholipid vesicles with planar bilayer membranes. *J. Cell. Biol.* **1984**, *98*, 1054–1062.
[24] Kuzmin, P. I.; Zimmerberg, J.; Chizmadzhev, Y. A.; Cohen, F. S. A quantitative model for membrane fusion based on low-energy intermediates. *Proc. Natl. Acad. Sci. U. S. A.* **2001**, *98*, 7235–7240.
[25] Nanavati, C.; Markin, V. S.; Oberhauser, A. F.; Fernandez, J. M. The exocytotic fusion pore modeled as a lipidic pore. *Biophys. J.* **1992**, *63*, 1118–1132.
[26] Llinas, R. R. Calcium in synaptic transmission. *Sci. Am.* **1982**, *247*, 56–65.
[27] Sabatini, B. L.; Regehr, W. G. Timing of neurotransmission at fast synapses in the mammalian brain. *Nature* **1996**, *384*, 170–172.
[28] Rettig, J.; Neher, E. Emerging roles of presynaptic proteins in Ca^{++}-triggered exocytosis. *Science* **2002**, *298*, 781–785.
[29] Martens, S.; Kozlov, M. M.; McMahon, H. T. How synaptotagmin promotes membrane fusion. *Science* **2007**, *316*, 1205–1208.
[30] Eberhard, D. A.; Cooper, C. L.; Low, M. G.; Holz, R. W. Evidence that the inositol phospholipids are necessary for exocytosis. Loss of inositol phospholipids and inhibition of secretion in permeabilized cells caused by a bacterial phospholipase C and removal of ATP. *Biochem. J.* **1990**, *268*, 15–25.
[31] Peppers, S. C.; Holz, R. W. Catecholamine secretion from digitonin-treated PC12 cells. Effects of Ca^{2+}, ATP, and protein kinase C activators. *J. Biol. Chem.* **1986**, *261*, 14665–14669.
[32] Aikawa, Y.; Martin, T. F. ARF6 regulates a plasma membrane pool of phosphatidylinositol(4,5)bisphosphate required for regulated exocytosis. *J. Cell. Biol.* **2003**, *162*, 647–659.
[33] Holz, R. W.; Hlubek, M. D.; Sorensen, S. D.; Fisher, S. K.; Balla, T.; Ozaki, S.; Prestwich, G. D.; Stuenkel, E. L.; Bittner, M. A. A pleckstrin homology domain specific for PtdIns-4-5-P 2 and fused to green fluorescent protein identifies plasma membrane PtdIns-4-5-P 2 as being important in exocytosis. *J. Biol. Chem.* **2000**, *275*, 17878–17885.
[34] Routt, S. M.; Ryan, M. M.; Tyeryar, K.; Rizzieri, K. E.; Mousley, C.; Roumanie, O.; Brennwald, P. J.; Bankaitis, V. A. Nonclassical PITPs activate PLD via the Stt4p PtdIns-4-kinase and modulate function of late stages of exocytosis in vegetative yeast. *Traffic* **2005**, *6*, 1157–1172.
[35] He, B.; Xi, F.; Zhang, X.; Zhang, J.; Guo, W. Exo70 interacts with phospholipids and mediates the targeting of the exocyst to the plasma membrane. *Embo. J.* **2007**, *26*, 4053–4065.
[36] Di Paolo, G.; De Camilli, P. Phosphoinositides in cell regulation and membrane dynamics. *Nature* **2006**, *443*, 651–657.
[37] Murray, D. H.; Tamm, L. K. Clustering of syntaxin-1A in model membranes is modulated by phosphatidylinositol 4,5-bisphosphate and cholesterol. *Biochemistry.* **2009**, *48*, 4617–4625.
[38] Qiao, H.; Armstrong, R. T.; Melikyan, G. B.; Cohen, F. S.; White, J. M. A specific point mutant at position 1 of the influenza hemagglutinin fusion peptide displays a hemifusion phenotype. *Mol. Biol. Cell.* **1999**, *10*, 2759–2769.
[39] Wilson, I. A.; Skehel, J. J.; Wiley, D. C. Structure of the haemagglutinin membrane glycoprotein of influenza virus at 3 A resolution. *Nature* **1981**, *289*, 366–373.
[40] Bullough, P. A.; Hughson, F. M.; Skehel, J. J.; Wiley, D. C. Structure of influenza haemagglutinin at the pH of membrane fusion. *Nature* **1994**, *371*, 37–43.
[41] Copeland, C. S.; Zimmer, K. P.; Wagner, K. R.; Healey, G. A.; Mellman, I.; Helenius, A. Folding, trimerization, and transport are sequential events in the biogenesis of influenza virus hemagglutinin. *Cell* **1988**, *53*, 197–209.
[42] Skehel, J. J.; Wiley, D. C. Receptor binding and membrane fusion in virus entry: the influenza hemagglutinin. *Annu. Rev. Biochem.* **2000**, *69*, 531–569.
[43] Han, X.; Bushweller, J. H.; Cafiso, D. S.; Tamm, L. K. Membrane structure and fusion-triggering conformational change of the fusion domain from influenza hemagglutinin. *Nat. Struct. Biol.* **2001**, *8*, 715–720.
[44] Huang, Q.; Opitz, R.; Knapp, E. W.; Herrmann, A. Protonation and stability of the globular domain of influenza virus hemagglutinin. *Biophys. J.* **2002**, *82*, 1050–1058.
[45] Huang, Q.; Sivaramakrishna, R. P.; Ludwig, K.; Korte, T.; Bottcher, C.; Herrmann, A. Early steps of the conformational change of influenza virus hemagglutinin to a fusion active state: stability and energetics of the hemagglutinin. *Biochim. Biophys. Acta* **2003**, *1614*, 3–13.

[46] Rachakonda, P. S.; Veit, M.; Korte, T.; Ludwig, K.; Bottcher, C.; Huang, Q.; Schmidt, M. F.; Herrmann, A. The relevance of salt bridges for the stability of the influenza virus hemagglutinin. *Faseb. J.* **2007**, *21*, 995–1002.

[47] Chen, J.; Wharton, S. A.; Weissenhorn, W.; Calder, L. J.; Hughson, F. M.; Skehel, J. J.; Wiley, D. C. A soluble domain of the membrane-anchoring chain of influenza virus hemagglutinin (HA2) folds in *Escherichia coli* into the low-pH-induced conformation. *Proc. Natl. Acad. Sci. U. S. A.* **1995**, *92*, 12205–12209.

[48] Andres, D. A.; Seabra, M. C.; Brown, M. S.; Armstrong, S. A.; Smeland, T. E.; Cremers, F. P.; Goldstein, J. L. cDNA cloning of component A of Rab geranylgeranyl transferase and demonstration of its role as a Rab escort protein. *Cell* **1993**, *73*, 1091–1099.

[49] Qiao, H.; Pelletier, S. L.; Hoffman, L.; Hacker, J.; Armstrong, R. T.; White, J.M. Specific single or double proline substitutions in the "spring-loaded" coiled-coil region of the influenza hemagglutinin impair or abolish membrane fusion activity. *Cell. Biol.* **1998**, *141*, 1335–1347.

[50] Gruenke, J. A.; Armstrong, R. T.; Newcomb, W. W.; Brown, J. C.; White, J.M. New insight into the spring-loaded conformational change of influenza virus hemagglutinin. *J. Virol.* **2002**, *76*, 4456–4466.

[51] Park, H. E.; Gruenke, J. A.; White, J. M. Leash in the groove mechanism of membrane fusion. *Nat. Struct. Biol.* **2003**, *10*, 1048–1053.

[52] Han, X.; Tamm, L. K. A host-guest system to study structure-function relationships of membrane fusion peptides. *Proc. Natl. Acad. Sci. U. S. A.* **2000**, *97*, 13097–13102.

[53] Chernomordik, L. V.; Leikina, E.; Kozlov, M. M.; Frolov, V. A.; Zimmerberg, J. Structural intermediates in influenza haemagglutinin-mediated fusion. *J. Mol. Membr. Biol.* **1999**, *16*, 33–42.

[54] Cross, K. J.; Langley, W. A.; Russell, R. J.; Skehel, J. J.; Steinhauer, D. A. Composition and functions of the influenza fusion peptide. *Protein. Pept. Lett.* **2009**, *16*, 766–778.

[55] Skehel, J. J.; Bizebard, T.; Bullough, P. A.; Hughson, F. M.; Knossow, M.; Steinhauer, D. A.; Wharton, S. A.; Wiley, D. C. Membrane fusion by influenza hemagglutinin. *Cold. Spring. Harb. Symp. Quant. Biol.* **1995**, *60*, 573–580.

[56] Gething, M. J.; Doms, R. W.; York, D.; White, J. Studies on the mechanism of membrane fusion: site-specific mutagenesis of the hemagglutinin of influenza virus. *J. Cell. Biol.* **1986**, *102*, 11–23.

[57] Tamm, L. K. Hypothesis: spring-loaded boomerang mechanism of influenza hemagglutinin-mediated membrane fusion. *Biochim. Biophys. Acta* **2003**, *1614*, 14–23.

[58] Zwilling, D.; Cypionka, A.; Pohl, W. H.; Fasshauer, D.; Walla, P. J.; Wahl, M. C.; Jahn, R. Early endosomal SNAREs form a structurally conserved SNARE complex and fuse liposomes with multiple topologies. *EMBO. J.* **2007**, *26*, 9–18.

[59] Abrahamyan, L. G.; Mkrtchyan, S. R.; Binley, J.; Lu, M.; Melikyan, G. B.; Cohen, F. S. The cytoplasmic tail slows the folding of human immunodeficiency virus type 1 Env from a late prebundle configuration into the six-helix bundle. *J. Virol.* **2005**, *79*, 106–115.

[60] Lai, A. L.; Park, H.; White, J. M.; Tamm, L. K. Fusion peptide of influenza hemagglutinin requires a fixed angle boomerang structure for activity. *J. Biol. Chem.* **2006**, *281*, 5760–5770.

[61] Lai, A. L.; Tamm, L. K. Locking the kink in the influenza hemagglutinin fusion domain structure. *J. Biol. Chem.* **2007**, *282*, 23946–23956.

[62] Danieli, T.; Pelletier, S. L.; Henis, Y. I.; White, J. M. Membrane fusion mediated by the influenza virus hemagglutinin requires the concerted action of at least three hemagglutinin trimers. *J. Cell. Biol.* **1996**, *133*, 559–569.

[63] Frolov, V. A.; Cho, M. S.; Bronk, P.; Reese, T. S.; Zimmerberg, J. Multiple local contact sites are induced by GPI-linked influenza hemagglutinin during hemifusion and flickering pore formation. *Traffic* **2000**, *1*, 622–630.

[64] Tatulian, S. A.; Tamm, L. K. Secondary structure, orientation, oligomerization, and lipid interactions of the transmembrane domain of influenza hemagglutinin. *Biochemistry* **2000**, *39*, 496–507.

[65] Le Blanc, I.; Luyet, P. P.; Pons, V.; Ferguson, C.; Emans, N.; Petiot, A.; Mayran, N.; Demaurex, N.; Faure, J.; Sadoul, R.; Parton, R. G.; Gruenberg, J. Endosome-to-cytosol transport of viral nucleocapsids. *J. Nat. Cell. Biol.* **2005**, *7*, 653–664.

[66] Puri, A.; Booy, F. P.; Doms, R. W.; White, J. M.; Blumenthal, R. Conformational changes and fusion activity of influenza virus hemagglutinin of the H2 and H3 subtypes: effects of acid pretreatment. *J. Virol.* **1990**, *64*, 3824–3832.

[67] Tatulian, S. A.; Tamm, L. K. Reversible pH-dependent conformational change of reconstituted influenza hemagglutinin. *J. Mol. Biol.* **1996**, *260*, 312–316.

[68] Melikyan, G. B.; Lin, S.; Roth, M. G.; Cohen, F. S. Amino acid sequence requirements of the transmembrane and cytoplasmic domains of influenza virus hemagglutinin for viable membrane fusion. *Mol. Biol. Cell.* **1999**, *10*, 1821–1836.

[69] Jahn, R.; Scheller, R. H. SNAREs-energies for membrane fusion. *Nat. Rev. Mol. Cell. Biol.* **2006**, *7*, 631–643.

[70] Sutton, R. B.; Fasshauer, D.; Jahn, R.; Brunger, A. T. Crystal structure of a SNARE complex involved in synaptic exocytosis at 2.4 A resolution. *Nature* **1998**, *395*, 347–353.

[71] Li, F.; Pincet, F.; Perez, E.; Eng, W. S.; Melia, T. J.; Rothman, J. E.; Tareste, D. Energetics and dynamics of SNAREpin folding across lipid bilayers. *Nat. Struct. Mol. Biol.* **2007**, *14*, 890–896.

[72] Liu, W.; Parpura, V. Single molecule probing of SNARE proteins by atomic force microscopy. *Ann. N. Y. Acad. Sci.* **2009**, *1152*, 113–120.

[73] Wiederhold, K.; Fasshauer, D. Is assembly of the SNARE complex enough to fuel membrane fusion. *J. Biol. Chem.* **2009**, *284*, 13143–13152.

[74] Antonin, W.; Fasshauer, D.; Becker, S.; Jahn, R.; Schneider, T. R. Crystal structure of the endosomal SNARE complex reveals common structural principles of all SNAREs. *Nat. Struct. Biol.* **2002**, *9*, 107–111.

[75] Brunger, A. T. Q. Structure and function of SNARE and SNARE-interacting proteins. *Rev. Biophys.* **2005**, *38*, 1–47.

[76] Brunger, A. T. Structure of proteins involved in synaptic vesicle fusion in neurons. *Annu. Rev. Biophys. Biomol. Struct.* **2001**, *30*, 157–171.

[77] Ossig, R.; Schmitt, H. D.; de Groot, B.; Riedel, D.; Keranen, S.; Ronne, H.; Grubmuller, H.; Jahn, R. Exocytosis requires asymmetry in the central layer of the SNARE complex. *Embo. J.* **2000**, *19*, 6000–6010.

[78] Lauer, J. M.; Dalal, S.; Marz, K. E.; Nonet, M. L.; Hanson, P. I. SNARE complex zero layer residues are not critical for N-ethylmaleimide-sensitive factor-mediated disassembly. *J. Biol. Chem.* **2006**, *281*, 14823–14832.

[79] Katz, L.; Brennwald, P. Testing the 3Q:1R "rule": mutational analysis of the ionic "zero" layer in the yeast exocytic SNARE complex reveals no requirement for arginine. *Mol. Biol. Cell.* **2000**, *11*, 3849–3858.

[80] Wei, S.; Xu, T.; Ashery, U.; Kollewe, A.; Matti, U.; Antonin, W.; Rettig, J.; Neher, E. Exocytotic mechanism studied by truncated and zero layer mutants of the C-terminus of SNAP-25. *Embo. J.* **2000**, *19*, 1279–1289.

[81] Ellena, J. F.; Liang, B.; Wiktor, M.; Stein, A.; Cafiso, D. S.; Jahn, R.; Tamm, L. K. Dynamic structure of lipid-bound synaptobrevin suggests a nucleation-propagation mechanism for trans-SNARE complex formation. *Proc. Natl. Acad. Sci. U. S. A.* **2009**, *106*, 20306–20311.

[82] Su, Z.; Ishitsuka, Y.; Ha, T.; Shin, Y. K. The SNARE complex from yeast is partially unstructured on the membrane. *Structure* **2008**, *16*, 1138–1146.

[83] Pobbati, A. V.; Razeto, A.; Boddener, M.; Becker, S.; Fasshauer, D. Structural basis for the inhibitory role of tomosyn in exocytosis. *J. Biol. Chem.* **2004**, *279*, 47192–47200.

[84] Han, X.; Wang, C. T.; Bai, J.; Chapman, E. R.; Jackson, M. B. Transmembrane segments of syntaxin line the fusion pore of Ca^{2+}-triggered exocytosis. *Science* **2004**, *30i4*, 289–292.

[85] Domanska, M. K.; Kiessling, V.; Stein, A.; Fasshauer, D.; Tamm, L. K. Single vesicle millisecond fusion kinetics reveals number of SNARE complexes optimal for fast SNARE-mediated membrane fusion. *J. Biol. Chem.* **2009**, *284*, 32158–32166.

[86] Domanska, M. K.; Kiessling, V.; Tamm, L. K. Docking and fast fusion of synaptobrevin vesicles depends on the lipid compositions of the vesicle and the acceptor SNARE complex-containing target membrane. *Biophys. J* **2010**, *99*, 2936–2946.

[87] Ohya, T.; Miaczynska, M.; Coskun, U.; Lommer, B.; Runge, A.; Drechsel, D.; Kalaidzidis, Y.; Zerial, M. Reconstitution of Rab- and SNARE-dependent membrane fusion by synthetic endosomes. *Nature* **2009**, *459*, 1091–1097.

[88] Weninger, K.; Bowen, M. E.; Chu, S.; Brunger, A. T. Single-molecule studies of SNARE complex assembly reveal parallel and antiparallel configurations. *Proc. Natl. Acad. Sci. U. S. A.* **2003**, *100*, 14800–14805.

[89] Han, X.; Jackson, M. B. Structural transitions in the synaptic SNARE complex during Ca^{2+}-triggered exocytosis. *J. Cell. Biol.* **2006**, *172*, 281–293.

[90] Schiavo, G.; Poulain, B.; Benfenati, F.; DasGupta, B. R.; Montecucco, C. Novel targets and catalytic activities of bacterial protein toxins. *Trends. Microbiol.* **1993**, *1*, 170–174.

[91] Brunger, A. T.; Rummel, A. Receptor and substrate interactions of clostridial neurotoxins. *Toxicon* **2009**, *54*, 550–560.

[92] Bracher, A.; Kadlec, J.; Betz, H.; Weissenhorn, W. X-ray structure of a neuronal complexin-SNARE complex from squid. *J. Biol. Chem.* **2002**, *277*, 26517–26523.

[93] Chen, X.; Tomchick, D. R.; Kovrigin, E.; Arac, D.; Machius, M.; Sudhof, T. C.; Rizo, J. Three-dimensional structure of the complexin/SNARE complex. *Neuron* **2002**, *33*, 397–409.

[94] Fernandez-Chacon, R.; Wolfel, M.; Nishimune, H.; Tabares, L.; Schmitz, F.; Castellano-Munoz, M.; Rosenmund, C.; Montesinos, M. L.; Sanes, J. R.; Schneggenburger, R.; Sudhof, T. C. The synaptic vesicle protein CSP alpha prevents presynaptic degeneration. *Neuron* **2004**, *42*, 237–251.

[95] Sirkis, R.; Gerst, J. E.; Fass, D. Ddi1, a eukaryotic protein with the retroviral protease fold. *J. Mol. Biol.* **2006**, *364*, 376–387.

[96] Gabriely, G.; Kama, R.; Gelin-Licht, R.; Gerst, J. E. Different domains of the UBL-UBA ubiquitin receptor, Ddi1/Vsm1, are involved in its multiple cellular roles. *Mol. Biol. Cell.* **2008**, *19*, 3625–3637.

[97] Ren, Y.; Yip, C. K.; Tripathi, A.; Huie, D.; Jeffrey, P. D.; Walz, T.; Hughson, F. M. A structure-based mechanism for vesicle capture by the multisubunit tethering complex Dsl1. *Cell* **2009**, *139*, 1119–1129.

[98] Simonsen, A.; Gaullier, J. M.; D'Arrigo, A.; Stenmark, H. The Rab5 effector EEA1 interacts directly with syntaxin-6. *J. Biol. Chem.* **1999**, *274*, 28857–28860.

[99] Elazar, Z.; Scherz-Shouval, R.; Shorer, H. Involvement of LMA1 and GATE-16 family members in intracellular membrane dynamics. *Biochim. Biophys. Acta.* **2003**, *1641*, 145–156.

[100] Paz, Y.; Elazar, Z.; Fass, D. Structure of GATE-16, membrane transport modulator and mammalian ortholog of autophagocytosis factor Aut7p. *J. Biol. Chem.* **2000**, *275*, 25445–25450.

[101] Paumet, F.; Wesolowski, J.; Garcia-Diaz, A.; Delevoye, C.; Aulner, N.; Shuman, H. A.; Subtil, A.; Rothman, J. E. Intracellular bacteria encode inhibitory SNARE-like proteins. *PLoS One.* **2009**, *4*, e7375.

[102] Maruyama, I. N.; Brenner, S. A phorbol ester/diacylglycerol-binding protein encoded by the unc-13 gene of Caenorhabditis elegans. *Proc. Natl. Acad. Sci. U. S. A.* **1991**, *88*, 5729–5733.

[103] Richmond, J. E.; Weimer, R. M.; Jorgensen, E. M. An open form of syntaxin bypasses the requirement for UNC-13 in vesicle priming. *Nature* **2001**, *412*, 338–341.

[104] Rodriguez-Castaneda, F.; Maestre-Martinez, M.; Coudevylle, N.; Dimova, K.; Junge, H.; Lipstein, N.; Lee, D.; Becker, S.; Brose, N.; Jahn, O.; Carlomagno, T.; Griesinger, C. Modular architecture of Munc 13/calmodulin complexes: dual regulation by Ca^{2+} and possibility function in short-term synaptic plasticity. *Embo. J* **2010**, *29*, 680–691.

[105] Lu, J.; Machius, M.; Dulubova, I.; Dai, H.; Sudhof, T. C.; Tomchick, D. R.; Rizo, J. Structural basis for a Munc13-1 homodimer to Munc13-1/RIM heterodimer switch. *PLoS Biol.* **2006**, *4*, e192.

[106] Zhao, C.; Slevin, J. T.; Whiteheart, S. W. Cellular functions of NSF: not just SNAPs and SNAREs. *FEBS Lett.* **2007**, *581*, 2140–2149.

[107] Martincic, I.; Peralta, M. E.; Ngsee, J. K. Isolation and characterization of a dual prenylated Rab and VAMP2 receptor. *J. Biol. Chem.* **1997**, *272*, 26991–26998.

[108] Ostermeier, C.; Brunger, A. T. Structural basis of Rab effector specificity: crystal structure of the small G protein Rab3A complexed with the effector domain of rabphilin-3A. *Cell* **1999**, *96*, 363–374.

[109] Otto, G. P.; Razi, M.; Morvan, J.; Stenner, F.; Tooze, S. A. A novel syntaxin 6-interacting protein, SHIP164, regulates syntaxin 6-dependent sorting from early endosomes. *Traffic* **2010**, *11*, 688–705.

[110] Hata, Y.; Slaughter, C. A.; Sudhof, T. C. Synaptic vesicle fusion complex contains unc-18 homologue bound to syntaxin. *Nature* **1993**, *366*, 347–351.

[111] Pevsner, J.; Hsu, S. C.; Braun, J. E.; Calakos, N.; Ting, A. E.; Bennett, M. K.; Scheller, R. H. Specificity and regulation of a synaptic vesicle docking complex. *Neuron* **1994**, *13*, 353–361.

[112] Carr, C. M.; Grote, E.; Munson, M.; Hughson, F. M.; Novick, P. J. Sec1p binds to SNARE complexes and concentrates at sites of secretion. *J. Cell. Biol.* **1999**, *146*, 333–344.

[113] Fujita, Y.; Shirataki, H.; Sakisaka, T.; Asakura, T.; Ohya, T.; Kotani, H.; Yokoyama, S.; Nishioka, H.; Matsuura, Y.; Mizoguchi, A.; Scheller, R. H.; Takai, Y. Tomosyn: a syntaxin-1-binding protein that forms a novel complex in the neurotransmitter release process. *Neuron* **1998**, *20*, 905–915.

[114] Hattendorf, D. A.; Andreeva, A.; Gangar, A.; Brennwald, P. J.; Weis, W. I. Structure of the yeast polarity protein Sro7 reveals a SNARE regulatory mechanism. *Nature* **2007**, *446*, 567–571.

[115] Scales, S. J.; Hesser, B. A.; Masuda, E. S.; Scheller, R. H. Amisyn, a novel syntaxin-binding protein that may regulate SNARE complex assembly. *J. Biol. Chem.* **2002**, *277*, 28271–28279.

[116] Whiteheart, S. W.; Griff, I. C.; Brunner, M.; Clary, D. O.; Mayer, T.; Buhrow, S. A.; Rothman, J. E. SNAP family of NSF attachment proteins includes a brain-specific isoform. *Nature* **1993**, *362*, 353–355.

[117] Griff, I. C.; Schekman, R.; Rothman, J. E.; Kaiser, C. A. The yeast SEC17 gene product is functionally equivalent to mammalian alpha-SNAP protein. *J. Biol. Chem.* **1992**, *267*, 12106–12115.

[118] Groffen, A. J.; Martens, S.; Diez Arazola, R.; Cornelisse, L. N.; Lozovaya, N.; de Jong, A. P.; Goriounova, N. A.; Habets, R. L.; Takai, Y.; Borst, J. G.; Brose, N.; McMahon, H. T.; Verhage, M. Doc2b is a high affinity Ca^{2+} sensor for spontaneous neurotransmitter release. *Science* **2010**, *327*, 1614–1618.

[119] Wang, C. T.; Bai, J.; Chang, P. Y.; Chapman, E. R.; Jackson, M. B. Synaptotagmin-Ca^{2+} triggers two sequential steps in regulated exocytosis in rat PC12 cells: fusion pore opening and fusion pore dilation. *J. Physiol.* **2006**, *570*, 295–307.

[120] Wang, C. T.; Grishanin, R.; Earles, C. A.; Chang, P. Y.; Martin, T. F.; Chapman, E. R.; Jackson, M. B. Synaptotagmin modulation of fusion pore kinetics in regulated exocytosis of dense-core vesicles. *Science* **2001**, *294*, 1111–1115.

[121] Edelmann, L.; Hanson, P. I.; Chapman, E. R.; Jahn, R. Synaptobrevin binding to synaptophysin: a potential mechanism for controlling the exocytotic fusion machine. *Embo. J.* **1995**, *14*, 224–231.

[122] Calakos, N.; Scheller, R. H. Vesicle-associated membrane protein and synaptophysin are associated on the synaptic vesicle. *J. Biol. Chem.* **1994**, *269*, 24534–24537.

[123] Burre, J.; Sharma, M.; Tsetsenis, T.; Buchman, V.; Etherton, M. R.; Sudhof, T.C. Alpha-synuclein promotes SNARE-complex assembly *in vivo* and *in vitro*. *Science* **2010**, *329*, 1663–1667.

[124] Chandra, S.; Gallardo, G.; Fernandez-Chacon, R.; Schluter, O. M.; Sudhof, T.C. Alpha-synuclein cooperates with CSPalpha in preventing neurodegeneration. *Cell* **2005**, *123*, 383–396.

[125] Diao, J.; Su, Z.; Ishitsuka, Y.; Lu, B.; Lee, K. S.; Lai, Y.; Shin, Y. K.; Ha, T. A single-vesicle content mixing assay for SNARE-mediated membrane fusion. *Nat. Commun* **2010**, *1*, 1–6.

[126] Cypionka, A.; Stein, A.; Hernandez, J. M.; Hippchen, H.; Jahn, R.; Walla, P. J. Discrimination between docking and fusion of liposomes reconstituted with neuronal SNARE-proteins using FCS. *Proc. Natl. Acad. Sci. U. S. A.* **2009**, *106*, 18575–18580.

[127] Brunger, A. T.; Weninger, K.; Bowen, M.; Chu, S. Single-molecule studies of the neuronal SNARE fusion machinery. *Annu. Rev. Biochem.* **2009**, *78*, 903–928.

[128] Montana, V.; Liu, W.; Mohideen, U.; Parpura, V. Single molecule measurements of mechanical interactions within ternary SNARE complexes and dynamics of their disassembly: SNAP25 vs. SNAP23. *J. Physiol.* **2000**, *587*, 1943–1960.

[129] Liu, W.; Montana, V.; Bai, J.; Chapman, E. R.; Mohideen, U.; Parpura, V. Single molecule mechanical probing of the SNARE protein interactions. *Biophys. J.* **2006**, *91*, 744–758.

[130] Bowen, M. E.; Weninger, K.; Brunger, A. T.; Chu, S. Single molecule observation of liposome-bilayer fusion thermally induced by soluble N-ethyl maleimide sensitive-factor attachment protein receptors (SNAREs). *Biophys. J.* **2004**, *87*, 3569–3584.

[131] Lakadamyali, M.; Rust, M. J.; Babcock, H. P.; Zhuang, X. Visualizing infection of individual influenza viruses. *Proc. Natl. Acad. Sci. U. S. A.* **2003**, *100*, 9280–9285.

[132] Floyd, D. L.; Ragains, J. R.; Skehel, J. J.; Harrison, S. C.; van Oijen, A. M. Single-particle kinetics of influenza virus membrane fusion. *Proc. Natl. Acad. Sci. U. S. A.* **2008**, *105*, 15382–15387.

[133] Bashkirov, P. V.; Akimov, S. A.; Evseev, A. I.; Schmid, S. L.; Zimmerberg, J.; Frolov, V. A. GTPase cycle of dynamin is coupled to membrane squeeze and release, leading to spontaneous fission. *Cell* **2008**, *135*, 1276–1286.

[134] Pucadyil, T. J.; Schmid, S. L. Real-time visualization of dynamin-catalyzed membrane fission and vesicle release. *Cell* **2008**, *135*, 1263–1275.

[135] Kozlovsky, Y.; Kozlov, M. M. Membrane fission: model for intermediate structures. *Biophys. J.* **2003**, *85*, 85–96.

[136] Warnock, D. E.; Hinshaw, J. E.; Schmid, S. L. Dynamin self-assembly stimulates its GTPase activity. *J. Biol. Chem.* **1996**, *271*, 22310–22314.

[137] Ramachandran, R.; Schmid, S. L. Real-time detection reveals that effectors couple dynamin's GTP-dependent conformational changes to the membrane. *Embo. J.* **2008**, *27*, 27–37.

[138] Anantharam, A.; Bittner, M. A.; Aikman, R. L.; Stuenkel, E. L.; Schmid, S. L.; Axelrod, D.; Holz, R. W. A new role for the dynamin GTPase in the regulation of fusion pore expansion. *Mol. Biol. Cell.* **2011**, *22*, 1907–1918.

[139] Anantharam, A.; Onoa, B.; Edwards, R. H.; Holz, R. W.; Axelrod, D. Localized topological changes of the plasma membrane upon exocytosis visualized by polarized TIRFM. *J. Cell. Biol.* **2010**, *188*, 415–428.